

A Time-Domain Numerical Study of Passive and Active Anti-Roll Tanks to Reduce Ship Motions

Thomas W. Treakle, III

Thesis submitted to the Faculty of the Virginia Polytechnic Institute and State University in partial fulfillment of the requirements for the degree of

Master of Science
in
Ocean Engineering

Dean Mook, Chair
Sergios Liapis, Co-Chair
Ali Nayfeh
Wayne Neu

April 21, 1998
Blacksburg, VA

Keywords: Stabilizing Devices, Roll Motion, Anti-roll Tank, Ship, Control

A Time-Domain Numerical Study of Passive and Active Anti-Roll Tanks to Reduce Ship Motions

Thomas W. Treakle, III

(ABSTRACT)

Time-domain simulations were performed to investigate the influence of passive and active anti-roll tanks and moving weights on ship motions. A point mass moving across the ship was used to model the non-linear effects of the tank systems in various computer simulation environments. PID control of the mass position was used for the active tank (pump) systems and a vibration absorber was used for the passive tank systems. A single-degree-of-freedom non-linear code was developed to investigate the influence of various coefficients and control strategies. The final active and passive tank system implementations were included in the LAMP code developed by SAIC. Results of the time-domain simulations are shown, which indicate the effectiveness of these types of roll control systems.

ACKNOWLEDGMENTS

The work contained in this paper could not have been performed without the direct influence of several people. First a special thanks to God for granting me the ability, the opportunity, and the courage to undertake this work. My family has also been a source of encouragement and helped me persevere through the difficult emotional times I endured over the last year. Dr. Liapis and Dr. Mook were both instrumental in the formulation and revision of this thesis. Their comments and suggestions kept me on the right track. Randy Soper was of great help in the control theory area, and Dr. Nayfeh gave excellent advice on the formulation of the passive tank system and the development of MOTSIM. I'd also like to extend a thank you to John Martin of Flume Stabilization Systems and Bob Hatten of JJMA for helping me research the current industrial state of anti-roll tank systems. I would like to extend a special thanks to the Office of Naval Research for providing the funding for this research in the MURI on Nonlinear Control of Dynamical Systems. Lastly, a world of thanks goes to the crew at SAIC's Ship Technology Division for giving invaluable input, suggestions, and the necessary time and support to finish this work. I am indeed blessed by the opportunity to work with the leaders in the computational ship motions world: Nils Salvesen, Woei-Min Lin, Ken Weems, Sheguang Zhang, Mike Meinhold, Rich Korpus, Brian Hubbard, and Paul Jones. Thank you all.

TABLE OF CONTENTS

| | |
|---|------|
| ACKNOWLEDGMENTS | II |
| TABLE OF CONTENTS..... | III |
| LIST OF FIGURES..... | VI |
| LIST OF TABLES | VIII |
| LIST OF SYMBOLS..... | IX |
| <i>CHAPTER 1</i> INTRODUCTION..... | 1 |
| 1.1 Motivation for the Present Study | 1 |
| 1.2 Numerical Methods to Predict Ship Motions | 1 |
| 1.3 History of Roll Control Devices | 2 |
| 1.4 Survey of Related Literature..... | 3 |
| 1.5 Outline of Approach..... | 5 |
| <i>CHAPTER 2</i> DESCRIPTION OF LAMP SIMULATOR..... | 6 |
| 2.1 Theory and Assumptions | 6 |
| 2.2 Mathematical Formulation (Ref. LAMP version 2.83 Manual) | 7 |
| 2.3 Roll Damping Forces in LAMP | 10 |
| <i>CHAPTER 3</i> PASSIVE AND ACTIVE ANTI-ROLL TANK SYSTEMS..... | 11 |
| 3.1 General Assumptions | 11 |
| 3.2 Formulation of Active System in Reduced Model in LAMP..... | 11 |
| 3.2.1 Theory and Assumptions | 11 |
| 3.2.2 Mathematical Formulation | 12 |
| 3.2.2.1 Forces Added to the Equations of Motion for the Ship | 12 |
| 3.2.2.2 Servo Equation Specifying the Position of the Mass | 13 |
| 3.3 Formulation of the Active System for Six-Degree-of-Freedom Motion..... | 13 |
| 3.3.1 System Theory and Assumptions | 13 |
| 3.3.2 Mathematical Formulation | 14 |
| 3.4 Formulation of Passive Anti-Roll Tank System in Six Degrees of Freedom..... | 15 |
| 3.4.1 Theory and Assumptions | 15 |
| 3.4.2 Mathematical Formulation | 16 |

| | |
|--|-----------|
| CHAPTER 4 SINGLE-DEGREE-OF-FREEDOM SIMULATOR (MOTSIM) | 17 |
| 4.1 Motivation for Simulator, Theory, and Assumptions | 17 |
| 4.2 MOTSIM Mathematical Formulation | 17 |
| 4.2.1 Approximation for Ship Roll Equation of Motion | 17 |
| 4.2.2 Active and Passive System Motion | 18 |
| 4.2.3 Solution Technique | 18 |
| CHAPTER 5 RESULTS | 19 |
| 5.1 Ship Type and Configuration Used in Analysis of Tank Systems | 19 |
| 5.2 Theory and System Study Using MOTSIM | 20 |
| 5.2.1 Tuning MOTSIM to Match the LAMP Simulation | 20 |
| 5.2.2 Active-System Implementation | 22 |
| 5.2.2.1 Classic Approach for Controller Coefficient | 22 |
| 5.2.2.2 Initial Displacement Case | 23 |
| 5.2.2.3 Motion with Sinusoidal Forcing Function | 24 |
| 5.2.3 Passive System Implementation | 27 |
| 5.2.3.1 Initial Displacement Case | 27 |
| 5.2.3.2 Motion with Sinusoidal Forcing Function | 28 |
| 5.2.4 Coefficient Influence Study | 29 |
| 5.3 Installation of a Two-Degree-of-Freedom Active System in LAMP | 32 |
| 5.3.1 Ship Response, Without Roll Control | 32 |
| 5.3.2 Initial Displacement Case | 35 |
| 5.3.3 Forced Motion Case (Beam Sea) | 36 |
| 5.4 Installation of the Six-Degree-of-Freedom Systems in LAMP | 38 |
| 5.4.1 Active System Implementation | 38 |
| 5.4.1.1 Initial Displacement Case | 38 |
| 5.4.1.2 Forced Motion (Beam Sea) Case | 39 |
| 5.4.2 Passive System Implementation | 41 |
| 5.4.2.1 Initial Displacement Case | 41 |
| 5.4.2.2 Forced Motion (Beam Sea) Case | 42 |
| 5.4.3 Six-Degree-of-Freedom vs. Two-Degree-of Freedom LAMP Models | 44 |
| CHAPTER 6 CONCLUSIONS AND RECOMMENDATIONS FOR FUTURE WORK | 46 |
| 6.1 MOTSIM Anti-Roll Tank System Evaluation | 46 |
| 6.1.1 Active Anti-Roll-Tank System in MOTSIM | 46 |
| 6.1.2 Passive Anti-Roll Tank Systems in MOTSIM | 46 |
| 6.1.3 MOTSIM Coefficient Influence Study | 47 |
| 6.1.4 Recommendations for Future Development | 47 |
| 6.2 LAMP Anti-Roll Tank System Evaluation | 48 |
| 6.2.1 Active Anti-Roll Tank Systems in LAMP | 48 |
| 6.2.2 Passive Anti-Roll Tank Systems in LAMP | 49 |
| 6.2.3 Comparison of System Models | 49 |
| 6.2.4 Recommendations for Future Development | 50 |

| | |
|--|----|
| <i>CHAPTER 7</i> REFERENCES..... | 51 |
| APPENDIX A: SAMPLE INPUT FILE FOR SERIES 60, $C_B=0.7$ IN BEAM SEA | 54 |
| APPENDIX B: MOTSIM SOURCE CODE..... | 56 |
| APPENDIX C: LAMP NON-DIMENSIONALIZATION CHART | 60 |
| VITA..... | 61 |

LIST OF FIGURES

| | |
|---|----|
| Figure 2-1. LAMP Computational Domains..... | 8 |
| Figure 3-1. Anti-Roll Tank System..... | 11 |
| Figure 3-2. Initial Mass Motion Approximation..... | 12 |
| Figure 3-3. Coordinate System Diagram..... | 14 |
| Figure 5-1. Series 60, CB = 0.7 Cargo Ship Geometry and Panel Representation | 19 |
| Figure 5-2. Motion History of Initial Displacement Case in Calm Water Used to Tune MOTSIM to LAMP..... | 21 |
| Figure 5-3. System Block Diagram..... | 22 |
| Figure 5-4. System Root Locus and Zoomed Region..... | 23 |
| Figure 5-5. Motion History Following Release from an Initial Displacement for Two Cases: a) Ship Without Control b) Ship with Active Control where $m = 2\% M_{ship}$ | 24 |
| Figure 5-6. History of the Wave-Excited Motion for a Ship without Roll Control | 25 |
| Figure 5-7. History of the Wave-Excited Motion for a Ship with an Active Control System where $m = 2\% M_{ship}$ | 26 |
| Figure 5-8. Reduced Time History for a Wave-Excited Motion of a Ship with an Active Control System where $m = 2\% M_{ship}$ | 26 |
| Figure 5-9. Roll Histories Following an Initial Displacement and No Wave Excitation for Two MOTSIM Cases: a) Case without Control b) Case with Passive Control Where $m = 2\% M_{ship}$ | 27 |
| Figure 5-10. History of the Wave-Excited Motion of a Ship with a Passive-Control System where $m = 2\% M_{ship}$ | 28 |
| Figure 5-11. Reduced Time History for Wave-Excited Motion of a Ship with a Passive- Control System where $m = 2\% M_{ship}$ | 29 |
| Figure 5-12. Effect of Mass (m) on Steady-State Roll Amplitude, $z_m = 0.0$ | 30 |
| Figure 5-13. Effect of Z_m on Steady-State Roll Amplitude, $m = 2\% M_{ship}$ | 31 |
| Figure 5-14. Effect of d_{max} on Steady-State Roll Amplitude, $m = 2\% M_{ship}$, $z_m = 0.0$ | 32 |
| Figure 5-15. History from LAMP Calculation for a Ship Following an Initial Displacement in Roll without Control | 33 |
| Figure 5-16. History of the Wave-Excited Motion from LAMP Calculation for a Ship without Roll Control | 34 |
| Figure 5-17. History of Course-Keeping Rudder Motion for a Wave-Excited Ship without Roll Control..... | 34 |
| Figure 5-18. Roll Histories for 3 Cases Following an Initial Displacement with No Wave Excitation for the 2 Degree-of-Freedom Active-Tank Approximation | 35 |
| Figure 5-19. Wave-Excited Roll History from LAMP Calculation for the 2 Degree-of- Freedom Active-Tank Approximation | 37 |
| Figure 5-20. Roll Motion History from LAMP Calculation for a Ship with Active Anti-Roll Tanks Following Release from an Initial Displacement in Calm Water | 38 |
| Figure 5-21. History of the Wave-Excited Motion from LAMP Calculation for a Ship with Active Anti-Roll Tanks..... | 40 |
| Figure 5-22. Roll Motion History from LAMP Calculation of a Ship with Passive Anti-Roll Tanks Following Release from an Initial Displacement in Calm Water | 42 |
| Figure 5-23. History of the Wave-Excited Motion from LAMP Calculation for a Ship with Passive Anti-Roll Tanks..... | 43 |

Figure 5-24. History of the Wave-Excited Roll Motions from LAMP Calculations for a Ship with Six and Two Degree-of-Freedom Active Tank Formulations..... 44

Figure 5-25. History of the Wave Excited Roll Motions from LAMP Calculations for a Ship with Six and Two Degree-of-Freedom Passive Tank Formulations 45

LIST OF TABLES

| | |
|---|----|
| Table 5-1. Series 60, $C_B = 0.7$ Parameters and Specifications | 19 |
| Table 6-1. Roll Reduction Percentages for Systems in Wave-Excited Conditions where $m = 2\% M_{ship}$ | 50 |

LIST OF SYMBOLS

LAMP Formulation

| | | |
|------------|---|--|
| L | = | Ship Length |
| Φ_T | = | Total velocity potential |
| Φ_I | = | Potential of incident wave |
| Φ | = | Total disturbance potential |
| \vec{x} | = | Position vector of coordinate frame |
| g | = | Acceleration of gravity |
| v | = | Fluid domain |
| t | = | Time |
| τ | = | Time integration variable for previous steps |
| F | = | Mean free surface |
| B | = | Instantaneous body boundary |
| \vec{n} | = | Normal vector positive out of fluid domain |
| V_n | = | Instantaneous component of velocity of the ship in the direction normal to the surface of the hull |
| S_∞ | = | Infinity boundary of the fluid domain |
| P | = | Source points |
| Q | = | Field points |
| r | = | Distance to P |
| G | = | Velocity potential for step function source |
| G^o | = | Rankine potential |
| G^f | = | Free surface memory potential |
| J_0 | = | Bessel function of order zero |
| k | = | Wave number |
| σ | = | Wave angular frequency |
| Γ | = | Instantaneous intersection of the body with the free surface |
| \vec{N} | = | Unit normal to Γ |

LAMP Roll Damping Formulation

| | | |
|-----------|---|---|
| V_n | = | Velocity normal to the appendage |
| C | = | Chord length of appendage |
| \hat{c} | = | Chordwise vector on appendage |
| S | = | Span length of appendage |
| \hat{s} | = | Spanwise vector on appendage |
| Re | = | Reynolds number |
| C_N | = | Coefficient of normal pressure |
| C_A | = | Normal Pressure magnification factor |
| C_S | = | Factor for bilge keels built up from flat plate |
| C_K | = | Hull form correction factor |

Anti-roll Tank Formulation in LAMP and MOTSIM

| | | |
|--------------------------|---|---|
| x | = | Ship surge position * |
| y | = | Ship sway position * |
| z | = | Ship heave position * |
| ϕ | = | Ship roll Euler angle * |
| θ | = | Ship pitch Euler angle * |
| ψ | = | Ship yaw Euler angle * |
| u | = | Ship surge velocity * |
| v | = | Ship sway velocity * |
| w | = | Ship heave velocity * |
| p | = | Ship roll angular velocity * |
| q | = | Ship pitch angular velocity * |
| r | = | Ship yaw angular velocity * |
| \mathbf{v} | = | Vector of ship velocities (u, v, w, p, q, r) * |
| $[M]_{RB}$ | = | Rigid body inertia matrix (including added mass) * |
| $[C]_{RB}$ | = | Coriolis and centripetal term matrix (including added mass) * |
| $\boldsymbol{\tau}_{RB}$ | = | Rigid body force vector * |
| m | = | Approximated mass of moving fluid |
| M_{ship} | = | Mass of ship |
| F | = | Forces from tank system |
| \mathbf{A} | = | Transformation matrix from ship-fixed coordinate system to global coordinate system |
| C_g | = | Ship center of gravity |
| d | = | Position of m |
| d_c | = | Commanded position of m |
| z_m | = | Vertical height of m above C_g |
| x_m | = | Longitudinal distance of m from C_g |
| μ | = | Servo damping coefficient |
| ω | = | Servo frequency |
| G_1, G_2, G_3 | = | Constants for PID control |
| \mathbf{g} | = | Vector or acceleration from gravity |
| \mathbf{O} | = | Origin of ship fixed system |
| \mathbf{r}_o | = | Position of origin (considered C_g) of ship fixed system in the inertial system |
| \mathbf{r}_m | = | Position of mass in ship fixed system |
| \mathbf{R}_m | = | Position of mass in global system |
| \mathbf{v}_o | = | Absolute velocity of point \mathbf{O} |
| \mathbf{a}_o | = | Acceleration of point \mathbf{O} |
| $\boldsymbol{\omega}$ | = | Angular velocity of ship |
| $\boldsymbol{\alpha}$ | = | Angular acceleration of ship |
| \mathbf{F}_s | = | Force exerted on ship by m |
| \mathbf{F}_m | = | Force exerted on m by ship |
| \mathbf{M}_o | = | Moment from m about point \mathbf{O} |

* Denotes notation borrowed from Fossen (1995)

Note: All Values are Non-Dimensionalized (See Appendix C)

Chapter 1 Introduction

1.1 Motivation for the Present Study

The motions of ships and the control of those motions have been the focal point of extensive research over the years. A ship in a seaway undergoes complex motions that may reduce the operational range of the ship and be uncomfortable or even dangerous for the crew. In certain circumstances, the captain may be forced to alter course or slow the ship to reduce large motions. This could produce undesirable mission limitations for military vessels and reduce profits for commercial vessels. Controlling the ship motion is of great interest to many parties in the marine field since motion control during station keeping or low-speed maneuvers may broaden the safe operational range of many vessels.

Many types of devices have been designed to reduce ship motions. For an example, anti-roll fins are used in cases of high ship speeds. The present work is a time-domain numerical study of one particular type of motion control device, the anti-roll tank. An anti-roll tank system utilizes the side-to-side motion of a fluid, such as water, to provide a force to counteract the excitation from the waves. The fluid motion reduces the roll angle of the ship and expands the operational regime of the vessel. Anti-roll tank systems may be of an active or passive nature and are described in more detail later in this paper (see section 3.1). This work also applies to the case of moving masses due to the nature of the approximate formulation and will be discussed in section 3.1. The primary motivation of this research is to provide a simulated environment for designers to establish the feasibility of various control strategies on various hull shapes in various sea states without the expense of model testing all design iterations.

1.2 Numerical Methods to Predict Ship Motions

Accuracy in the prediction of ship motions and the resulting hydrodynamic loads is of great importance to the ship design process. Accurate predictions of the motion are also necessary for the development of control methods. Early pioneers in the study of a body moving and interacting with waves, such as Froude (1868) and Mitchell (1898), had to rely on scale model testing to predict the motions of these bodies in given wave conditions. While yielding fairly good results, this has been and continues to be a very expensive portion of the design process. As a result of the increasing cost of model testing there is a very strong need for less expensive alternatives that can lead to a reduction in the amount of model testing required.

Advancements in computer technology have made the development of numerical techniques to study the motions of ships not only possible but cost effective. Computational work that once required the speed of a super-computer such as a Cray can now be performed on desktop workstations. In recent years, much research has been dedicated to developing an accurate ship motion model.

Initial forms of a numerical model for ship motion were linearized and formulated in the frequency domain. Motions were considered to be small and harmonic in time. This formulation left a boundary-value problem that was first solved by a strip theory approach (see for example Salvesen, Tuck, and Faltinsen (1970)) and later solved by a three dimensional approach of distributing singularities on the body surface (see Ming Chang

(1977)). Korsmeyer (1988) showed how effective the three-dimensional formulation could be for the stationary-offshore-structure problem.

A time-domain initial-value formulation can be used as an alternative to the frequency-domain approach. The basic theoretical result of this formulation may be found in the work by Finkelstein (1957) and Cummins (1962). The Green function specified in the time-dependant formulation satisfies the free-surface boundary condition and is much simpler than the ones in the frequency domain. It is also capable of handling arbitrary large-amplitude motions when the proper memory effects are taken into account. The linearized three-dimensional radiation problem without forward speed was formulated by Liapis (1986) and Korsmeyer (1988), and work on a general linearized three-dimensional formulation with constant forward speed was undertaken by King (1987), Beck & Liapis (1987), and King, Beck, & Magee (1988).

The Science Applications International Corporation (SIAC) has recently developed a Large Amplitude Motions Program (LAMP) which implements the time-domain approach in a slightly different manner that includes large amplitude motions as described by Lin & Yue(1993). The exact body boundary condition is applied to the instantaneous submerged portion of the hull while a linearized free-surface condition is applied on the incident wave surface. Results obtained from this formulation are more general than those obtained from previous methods. The LAMP program is used in the present study as a tool to develop control methodology for the case of a moderate speed ship in various sea conditions.

1.3 History of Roll Control Devices

There are numerous reasons for trying to control and reduce the motions of a ship. Excessive motions can interfere with the activities of the crew or passengers, reduce the combat readiness of naval vessels, cause the loss of containers on cargo vessels, and reduce the operational parameters of various ships. Over the years, many types of motion control or reduction devices have been devised. Most have been aimed at reducing roll motions since the force required to reduce roll is reasonably small compared to the weight of the ship. Moreover, roll is the largest and most undesirable component of ship motion. Various methods include gyroscopic stabilizers, anti-roll tanks, fins, moving weights, and active rudder control. Most of these methods first started as passive control and then evolved into active control.

Schlick (1904) suggested placing a large gyroscope to supply a torque to oppose the roll motions. The system was installed on a German torpedo boat on 1906, and observed by White who gave a favorable review in *Scientific American* in 1907. Sperry then began pursuing active control methods based on using a gyroscope to oppose the rolling motion which he later patented.

In 1875 Watts first introduced the anti-roll tank as a passive method of damping rolling motions. He utilized the motion of water located in connected tanks. The motion of the ship caused the water to move from tank to tank, and the tank connection was tuned such that the motion of the water resonated out of phase with the roll motion. Minorsky (1941) did further work, but the crews of vessels outfitted with these early tank systems reported high noise levels while in operation. A detailed analysis of passive tank systems was performed with favorable results by Vasta, Giddings, Taplin, and Stilwell (1961).

Hort and Rellstab first implemented active tank systems in the 1930's where air pressure was applied to the tanks to force the water back and forth. In the 1940's, Minorsky

used a pump system to move the water between tanks. The US Navy continued to use active tank systems on their medium to fast speed vessels until the 1970's where both applied pressure and valve control were utilized. Webster (1967) showed that the use of active anti-roll tanks, when applied with a simple control strategy, gave much better results than the passive systems.

Bilge keels or fins protruding from the hull of the ship increase the damping of the roll motion. However the size of passive fins must be extremely large in order to produce any significant effect, and so their use is limited. Active fin systems have been utilized since the earliest attempts by the English developer Wilson in 1890 and Motora in Japan in the early 1900's. The most significant advances came between World War I and World War II when Denny, Brown Brothers, and the Admiralty Research Lab in the UK began a joint effort to develop an active fin system. Their scheme used wing like appendages controlled by gyroscopes that measured roll position and roll rate. Active fin systems have a major drawback, however: the effect of the fins is negligible at slow forward speed.

In 1910, Cremieu originally tested moving weight systems. He used a 10-ton mass mounted on a curved track that was immersed in a solution of glycerin and water. The mass was free to move in the solution that helped dissipate the kinetic energy of the system. Unfortunately, the system was not tuned properly and the mass impacted the stops at either end of the tracks and created large shocks. Norden was granted a US patent for a similar scheme in 1929. The use of moving masses has not been fully explored until recent years due to the size of the mass necessary to obtain a significant reduction in rolling motion.

Baitis & Schmidt (1989) presented the use of rudder roll stabilization employed by the U.S. Navy on a DD-963 (Spruance) class destroyer. The rudder roll stabilizer utilized the roll moment generated by the large rudders on the ship to dampen the roll motion without drastically altering the ship's course. The installed systems produced reductions in roll motion of approximately 40%. The advantage of such a system is that no large additional systems need to be installed on the ship. The rudder roll stabilization system is still one of the primary roll control devices in use on U.S. Navy ships, yet it loses effectiveness at reduced speeds.

1.4 Survey of Related Literature

The use of computational techniques to evaluate ship motion stabilization has been explored to only a limited degree. Vasta, Giddings, Taplin, and Stilwell (1961) derived a set of equations in the frequency-domain to describe the dynamics of a ship fitted with a passive anti-roll tank system. However, they utilized approximation and simplification techniques to solve the equation of motion directly.

Bell & Walker (1966) examined active and passive fluid tank systems for stabilizing ship motions. The active system uses a motor to drive a propeller and several control valves on a centrally located tank. The motor receives a signal from a sensing unit, which sends a signal to the motor. The motor then drives a propeller to move fluid from one side of the ship to the other. The effects of a passive tank system (i.e. propeller not operating) are also reported. The paper discussed that much better roll reduction characteristics are achieved for the active system than for the passive system.

Webster (1967) presented an analysis of control activated anti-roll tank systems, where a "U" tube formulation was derived. The linear ship motion response was formulated and solved in the frequency domain. Webster also described the modeling of

the pump system used in the active system, and presented a roll acceleration feedback type of controller. The equations for the active anti-roll tank system were formulated with saturation effects in the time-domain and solved using Runge-Kutta integration. However, the ship response was still solved in the frequency domain and the tank influences on the roll, sway, and yaw degrees of freedom for the various test cases were presented. The active tank system showed favorable roll reduction characteristics as compared to the passive system.

Field & Martin (1975) performed an evaluation of passive U-tube and free surface roll stabilization systems. They described the physical effects of variation of several parameters including fluid height, longitudinal and transverse crossover duct lengths, and vertical tank placement. Simplified equations for the roll motion of the ship fitted with these stabilizing systems were presented in the time domain, but a direct solution technique was applied to find the resulting average ship roll angle. Both systems presented showed good motion reduction characteristics, but the U-tube configuration had only a limited range of operational stability.

Webster, Dalzell, & Barr (1988) discussed a prediction method for evaluating the performance of free-flooding ship anti-rolling tanks. A study in the effectiveness of these free-flooding tank systems was done for the USS *Midway*. The equations for the prediction method are presented in the frequency domain where the tank system influences the ship in only the sway, roll, and yaw degrees of freedom. The predictions for three degrees of freedom showed very good agreement with experimental data for the significant roll amplitude.

Sellers & Martin (1992) presented a comparison of various roll-stabilization systems, where bilge keels, passive tanks, active fins, and rudder roll stabilization were considered. Several considerations were made in reference to the use of a passive tank system. Among these considerations were evaluating the frequency over which the tank system was effective, the effect of the tank system on the overall ship stability, and whether the tank system was sufficiently damped to ensure a flat response. The general weight of a passive tank system was stated to be 1% to 2% of the ship displacement, and a 40% to 60% reduction in roll angle was found. The passive tank system was also effective over all speed ranges.

Chen, Shaw, Khalil, & Troesch (1996) presented a study of robust stabilization of large amplitude ship rolling in regular beam seas, where a nonlinear three-degree-of-freedom model for the ship motion was derived. They also designed a nonlinear state feedback controller, which was applied to active anti-roll tanks. The authors suggested that the nonlinear controller stabilized a ship system from capsizing, even in cases where a linear controller failed.

At the present time, only one company in the United States supports the installation and use of anti-roll tank systems. Flume Stabilization Systems of Montclair, NJ has installed hundreds of passive and semi-active tank stabilization systems on a wide variety of commercial and naval vessels, and they are considered the world leader in this area.

Another area of related motion stabilization is the area of building motion control. In recent years, the use of moving masses and fluid-tank systems have been used for stabilizing building motions from wind, earthquakes, and traffic vibrations. Inoue, Kanyama, & Kanaji (1994) presented a study of two buildings in Japan where moving masses were used to reduce vehicle-traffic-induced vibrations. They reported a 64% reduction in one building and a 71% reduction in the other. Tamura (1995) discussed a

study of the control tower at Nagasaki Airport, where a tuned liquid column damper (TLD) is in use to reduce the wind induced vibrations of the tower. The passive TLD system reduced the motions of the tower top by 35-50% depending on wind speed and direction. Additional information on current and future systems for active and passive control of building structures may be found in the September 1997 issue of *Journal of Engineering Mechanics*, Vol. 123, No. 9.

1.5 Outline of Approach

All of the computations shown in this research are done in the time-domain. Typical formulations for the anti-roll tank problem were in the frequency-domain; however, the frequency-domain does not allow for the prediction of numerous non-linear effects. The formulation for the anti-roll tank system in the time-domain will hopefully give the designer a tool which will predict the effects from these tank systems in an environment more closely related to the true environment of the sea.

Since the focus of this research is on slowly moving or stationary ships, the motion control devices implemented in the LAMP code are of types suitable to this environment. Specifically the effects of anti-roll tanks and moving-mass devices are investigated in the simulated environment of LAMP. These two roll control systems share the same basic principle of operation: they provide control authority by moving mass from one side of the ship to the other. For the purpose of evaluating the feasibility of passive and active tank systems in a time-domain simulation, the fluid in the tanks is approximated by a point mass.

In order to formulate these motion-control systems in LAMP, several implementations with various assumptions are derived and developed as part of an evolving and sometimes iterative process. The mass used in the control system can either be considered a physical mass (i.e. lead block etc.) or an approximation to the fluid in the anti-roll tank system. The control problem is developed in two basic formulations, the passive-motion approach and the active-motion approach. A simplified single degree of freedom simulator for the roll motion of the ship called MOTSIM is also developed to investigate the relative importance of various terms and control strategies in the completed system.

The MOTSIM program is used to establish the feasibility and formulation of a vibration absorber system that has an active and a passive mode. The passive system is tuned to the natural frequency of the ship in roll. This system establishes the feasibility for the passive anti-roll tank approximation. The active mode of MOTSIM is used to show that the tuning of a spring-mass system can be used as an approximation for an active anti-roll tank system. The spring and damping terms in this formulation are representative of valve adjustments or fluid pumps which adjust the frequency of oscillation and the motion of the fluid in the tank system.

To fully show the capabilities of the control systems, a final implementation of the active and passive vibration absorbers are included in the LAMP code. Many cases are investigated with various sea conditions, initial displacements, and system configurations. Results are compiled and comparisons of the various formulations are shown.

The purpose of this research is to show the feasibility of these control methods by implementing them in the time-domain simulation and to give the designer an additional low-cost alternative to investigate control methods of these types. It is not the intent of this research to develop sophisticated algorithms or control logic for these systems. All of the control theory implemented in this paper is of a "Classical Control Theory" nature.

Chapter 2 Description of LAMP Simulator

2.1 Theory and Assumptions

The time-domain potential-flow code LAMP is used to predict the large-amplitude motions of a surface-piercing rigid body in a prescribed or arbitrary seaway. The fluid is considered homogenous, incompressible, inviscid, and its motion is irrotational. Surface tension is not taken into account and the depth is considered infinite. The exact body boundary condition is applied on the submerged hull surface and a linearized free-surface condition is applied on the incident wave. The approximation is justified by the assumption that the body geometry is “slender” in the directions of the large-amplitude motions. The linearized free surface requires that the slope of the incident wave must be small (i.e. the wave height is at least one order of magnitude smaller than the wavelength). The body is three-dimensional, floating on the free surface, and undergoing arbitrary six-degree-of-freedom motions.

A boundary-element approach is used. In this formulation, the instantaneous wetted surface of the body is divided into a number of panels over which linearized transient free-surface sources are distributed. The problem is formulated in a global fixed coordinate system, which allows for arbitrary large-amplitude motions. In this method, a general and concise waterline integral term can be found to account for translations and distortions of the body waterplane. The diffraction is taken into account by adding the incident wave contribution to the body boundary condition. The hydrostatic and hydrodynamic forces are found, and then the rigid-body equations of motion are solved to update the position and orientation of the body at the next time step.

There are three different versions of LAMP: LAMP-4, LAMP-2, and LAMP-1. LAMP-4 is the complete large-amplitude version in which the 3-D velocity potential is calculated with a linearized free-surface condition being satisfied on the surface of the incident wave. The hydrodynamic and hydrostatic pressures are both computed on the instantaneous wetted surface of the hull below the incident wave. At each time step the program must re-panel the surface of the hull and re-evaluate the free-surface Green’s Function. In summary, LAMP-4 solves the free-surface boundary condition on the incident wave surface, computes the 3-D large-amplitude hydrodynamics, and computes the nonlinear restoring and Froude-Krylov wave forces. Due to the large computational resources necessary for this method, it is used sparingly here.

LAMP-2 uses a linear 3-D approach to compute the hydrodynamic portion of the pressure forces. LAMP-2 approximates the large amplitude motion effects by stretching the pressure field on the hull surface if necessary. The free-surface boundary condition is applied on the mean water surface, and the nonlinear restoring and Froude-Krylov forces are computed. The computational requirements for this version are approximately one tenth of those for the LAMP-4 version. The nonlinear motions found using this version of LAMP combined with the relatively small computational requirements make LAMP-2 the choice for the majority of this research.

LAMP-1 is the linearized version of the method used in LAMP-4. The free-surface boundary condition is satisfied on the undisturbed free-surface position, and the linear hydrostatic restoring and Froude-Krylov wave forces are utilized. This version has about the same computational requirements as the LAMP-2 version.

The LAMP programs have many additional features. In addition to calculating the motions of and loads on floating bodies with or without forward speed in the time domain, they can be used for the numerical solution of many sea-keeping-related problems. Their prediction capabilities include the following:

- Impulse response functions
- Wave resistance of ships in calm water or in waves
- Linear and nonlinear motions of vessels in waves
- Linear and nonlinear hydrodynamic forces
- Linear and nonlinear wave excitation forces
- Pressure distributions over the hull surfaces
- Linear and nonlinear wave loads
- Impact and whipping loads
- Nonlinear time-domain simulation of ship motions in large-amplitude waves

LAMP is currently regarded as the most nearly complete and fully functional ship-motions code available for time-domain calculations.

2.2 Mathematical Formulation (Ref. LAMP version 2.83 Manual)

A velocity potential describes the fluid motions

$$\Phi_T(\vec{x}, t) = \Phi_I(\vec{x}, t) + \Phi(\vec{x}, t) \quad [2.1]$$

where Φ_I is the potential of the incident wave, $\Phi = \Phi_T - \Phi_I$ is the total disturbance potential, t is time, and \vec{x} is the position vector in the ground-fixed coordinate frame. In the fluid domain $v(t)$, Φ satisfies Laplace's equation:

$$\nabla^2 \Phi = 0 \quad [2.2]$$

On the mean free surface $F(t)$, a linearized free-surface condition is imposed:

$$\Phi_{tt} + g\Phi_z = 0 \text{ on } F(t), \quad t > 0 \quad [2.3]$$

where g is the acceleration from gravity and the lower case subscripts on Φ denote derivatives with respect to the subscripted variable. The no-penetration condition is applied on the instantaneous body boundary $B(t)$:

$$\frac{\partial \Phi}{\partial n} = V_n - \frac{\partial \Phi_I}{\partial n} \text{ on } B(t), \quad t > 0 \quad [2.4]$$

where the unit normal vector \vec{n} is positive out of the fluid domain and V_n is the instantaneous component of the velocity of the ship in the direction normal to the surface of the hull. For finite time, the conditions at infinity S_∞ are:

$$\Phi, \Phi_t = 0 \text{ on } S_\infty, \quad t > 0 \quad [2.5]$$

which are considered the radiation conditions.

The initial conditions are:

$$\Phi, \Phi_t = 0 \text{ on } F(t), \quad t = 0 \quad [2.6]$$

Now a transient free-surface Green's function describing the velocity potential for a step-function source below the free surface is introduced from Stoker (1957):

$$G(P, t, Q, \tau) = G^0 + G^f = \frac{1}{r} - \frac{1}{r'} + 2 \int_0^\infty [1 - \cos(\sqrt{gk}(t - \tau))] e^{k(z+\zeta)} J_0(kR) dk \quad [2.7]$$

for $P \neq Q, \quad t \geq \tau$

where $P = (x, y, z)$ and $Q = (\xi, \eta, \zeta)$ are the source and field points, $r = |P-Q|$, $r' = |P-Q'|$, $Q' = (\xi, \eta, -\zeta)$, $R^2 = (x - \xi)^2 + (y - \eta)^2$, $G^0 = 1/r - 1/r'$ is the Rankine part of the Green's function, $G^f = G - G^0$ is the free-surface memory, and J_0 is the Bessel function of order zero.

Equation [2.7] satisfies the following initial-boundary-value problem as follows:

$$\begin{aligned} \nabla^2 G &= 0 & \text{in } v(t), t > \tau \\ G_{tt} + gG_z &= 0 & \text{on } F(t), t > \tau \\ G, G_t &\rightarrow 0 & \text{for } t > \tau \\ G = G_t &= 0 & \text{on } F(t), t = \tau \end{aligned}$$

Please note that $G_\tau^0 = 0$ so that

$$G_\tau = G_\tau^f = -2 \int_0^\infty \sqrt{gk} \sin(\sqrt{gk}(t - \tau)) e^{k(z+\zeta)} J_0(kR) dk \quad [2.8]$$

The boundary integral for Φ is obtained by applying Green's identity to $\Phi(Q, \tau)$ and $G_\tau(P, t; Q, \tau)$ in a fluid domain $\bar{v}(\tau)$ bounded by $\bar{F}(\tau), \bar{B}(\tau), S_\infty$, and a small surface S_p excluding point P :

$$\iiint_{\bar{v}(\tau)} (\Phi \nabla_Q^2 G_\tau - G_\tau \nabla_Q^2 \Phi) dV = \iint_{S_\infty + \bar{F}(\tau) + \bar{B}(\tau) + S_p} (\Phi G_{mQ} - G_\tau \Phi_{nQ}) dS \quad [2.9]$$

where $\bar{v}(\tau), \bar{F}(\tau)$, and $\bar{B}(\tau)$ are, respectively, $v(\tau), F(\tau)$, and $B(\tau)$ with the possible exclusion of point P . Figure 2-1 shows the complete computational domain.

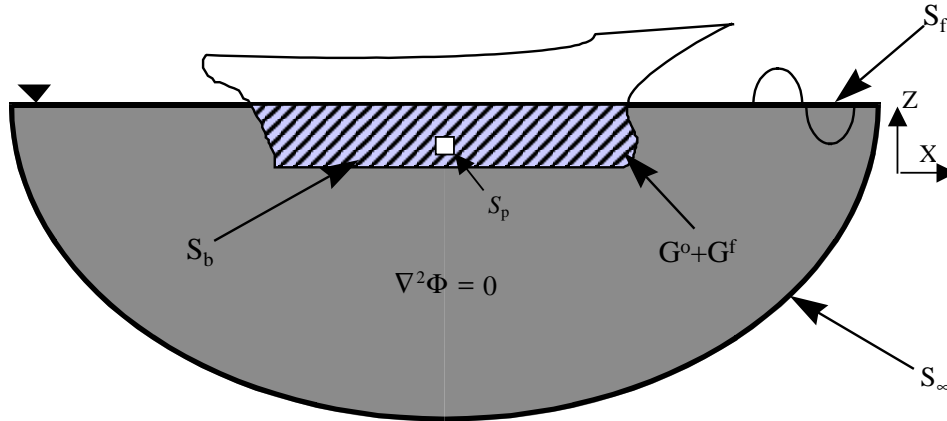


Figure 2-1. LAMP Computational Domains

The left-hand side of [2.9] and the integrals over S_∞ and S_p on the right-hand side are all equal to zero. By integrating the resulting equation with respect to τ from 0 to t we obtain the following form:

$$\int_0^t d\tau \iint_{\bar{F}(\tau) + \bar{B}(\tau)} (\Phi G_{mQ} - G_\tau \Phi_{nQ}) dS = 0 \quad [2.10]$$

In order to eliminate the integral over $\bar{F}(\tau)$, it is necessary to exchange the surface and time integrals involving $\bar{F}(\tau)$. $\bar{F}(\tau)$ is time-dependent in the earth-fixed coordinate system. After applying the linearized free-surface condition [2.3] and the transport theorem we obtain:

$$\iint_{\bar{F}(\tau)} (\Phi G_{mQ} - G_\tau \Phi_{nQ}) dS = -\frac{1}{g} \left\{ \frac{\partial}{\partial \tau} \iint_{\bar{F}(\tau)} (\Phi G_{\tau\tau} - G_\tau \Phi_\tau) dS - \int_{\bar{\Gamma}(\tau)} (\Phi G_{\tau\tau} - G_\tau \Phi_\tau) V_N dL \right\} \quad [2.11]$$

where $\bar{\Gamma}(\tau)$ is the instantaneous intersection of the body with the free surface excluding point P , \vec{N} is the unit normal to $\Gamma(\tau)$ on the free surface positive outward from the fluid domain, and V_N is the normal velocity of $\Gamma(\tau)$ in the \vec{N} direction. By combining [2.10] and [2.11], the initial conditions on Φ , and the free surface condition on G we obtain

$$\iint_{\bar{F}(\tau)} \Phi G_\tau^0 dS + \int_0^t d\tau \iint_{\bar{B}(\tau)} (\Phi G_{mQ} - G_\tau \Phi_{nQ}) dS + \frac{1}{g} \int_0^t d\tau \int_{\bar{\Gamma}(\tau)} (\Phi G_{\tau\tau} - G_\tau \Phi_\tau) V_N dL = 0 \quad [2.12]$$

If the Green's identity is applied to $\Phi(Q,t)$ and G^0 in $\bar{V}(t)$ and the result is combined with [2.12], the integral over the free surface $\bar{F}(\tau)$ can be eliminated. Now for point P on $B(t)$; the following expression for the velocity potential may be shown as

$$2\pi\Phi(P,t) + \iint_{B(t)} (\Phi G_{nQ}^0 - \Phi_{nQ} G^0) dS = \int_0^t d\tau \left\{ \iint_{B(\tau)} (\Phi G_{mQ}^f - \Phi_{nQ} G_\tau^f) dS + \frac{1}{g} \int_{\Gamma(\tau)} (\Phi G_{\tau\tau}^f - \Phi_\tau G_\tau^f) V_N dL \right\} \quad [2.13]$$

Because the integration over S_p gives no contribution, the over-bars on the limits of integration have been dropped. The waterline memory integral over $\Gamma(\tau)$ in [2.13] is in the general form for arbitrary large motions in the global earth-fixed coordinate system. For submerged bodies, this term goes to zero. For the special case of horizontal planar motion, this integral reduces to a term in the body-fixed coordinate system as given by Liapis [1986].

For large-amplitude problems, the tangential velocity evaluation on the body is critical, and in the absence of lift, a source formulation is preferred. The equation for the source formulation is found by formulating the interior problem which is governed by an equation similar to [2.13], which when combined with [2.13] gives:

$$\Phi(P,t) = -\frac{1}{4\pi} \left\{ \iint_{B(t)} (\sigma G^0) dS + \int_0^t \left[\iint_{B(\tau)} \sigma G_\tau^f dS - \frac{1}{g} \int_{\Gamma(\tau)} \sigma G_\tau^f V_N V_n dL \right] d\tau \right\} \quad [2.14]$$

where $\sigma(Q,t)$ is the source strength at time τ of point Q , and V_N and V_n are related by $V_N = V_n / \vec{N} \cdot \vec{n}$.

Now the body boundary condition for P on $B(t)$ may finally be applied to obtain:

$$\frac{\partial \Phi}{\partial n_p} = V_n(P,t) - \nabla \Phi_l(P,t) \cdot \vec{n}_p = -\frac{1}{4\pi} \left\{ \iint_{B(t)} \sigma G_{n_{pt}}^f dS + \int_0^t \left[\iint_{B(\tau)} \sigma G_{n_{pt}}^f dS - \frac{1}{g} \int_{\Gamma(\tau)} \sigma G_{n_{pt}}^f V_N V_n dL \right] d\tau \right\} \quad [2.15]$$

This equation can be solved for the unknown $\sigma(P,t)$ given $B(t)$, $V_n(t)$, $\Phi_l(t)$, $\sigma(P,\tau)$, and $B(\tau)$ for $0 \leq \tau < t$. Φ can be evaluated by [2.14] once the source strength is found. The velocity on the body, $\nabla \Phi$, is found by using the vector form of [2.15]. The formulation for the *general* arbitrary large-amplitude motions is now complete.

2.3 Roll Damping Forces in LAMP

Bilge keels are long plate-like appendages that are placed along the bilges of the ship to introduce roll damping. In LAMP, the forces from the bilge keels are included as eddy-making forces. The bilge keels have a fluid flow when the ship rolls which is normal to its surface, and the eddy-making force is calculated as the force on a flat plate in a flow normal to its surface. This is the time-domain equivalent of the semi-empirical method developed by Kato (1966)

To compute the eddy-making force, the normal component of the inflow is computed as

$$V_n = \vec{V}_r \cdot (\hat{c} \times \hat{s}) \quad [2.16]$$

where \hat{c} is a chord-wise unit vector and \hat{s} is a span-wise unit vector. The Reynolds number based on the span is

$$\text{Re} = \frac{V_n S}{\nu} \quad [2.17]$$

where S is the span distance and ν is the kinematic viscosity of water. A ‘‘coefficient of normal pressure’’, C_N , and ‘‘normal pressure magnification’’, C_A , are calculated (after Kato) as

$$\begin{aligned} C_N &= 1.98^{-11\frac{S}{c}} \text{ for } \frac{S}{C} < 0.07 \\ C_N &= 1.98^{-11\frac{C}{S}} \text{ for } \frac{S}{C} > \frac{1}{0.07} \\ C_N &= 1.18 \quad \text{for } 0.07 \leq \frac{S}{C} \leq \frac{1}{0.07} \end{aligned} \quad [2.18]$$

and

$$\begin{aligned} C_A &= 1.95 - 0.25 \ln(\text{Re}) + 0.20 \sin\left(\frac{\pi}{0.54} (\ln(\text{Re}) - 2.19)\right) \text{ for } \text{Re} < 1000 \\ C_A &= 1.0 \quad \text{for } \text{Re} \geq 1000 \end{aligned} \quad [2.19]$$

The hull form correction, C_K , and the factor for bilge keels built up from plates, C_S , are both set to 1.0. The normal or eddy-making force is then calculated as

$$\vec{F}_{eddy} = \frac{1}{2} C_N C_S C_A C_K \rho V_N^2 S C (\hat{c} \times \hat{s}) \quad [2.20]$$

Chapter 3 Passive and Active Anti-Roll Tank Systems

3.1 General Assumptions

Passive and active anti-roll tank systems operate on the principle that a fluid, usually water, moves from one tank to another and generates a moment on the ship that counteracts the motion. These two tanks are located as far out on the beam of the ship as possible to give the largest moment arm possible.

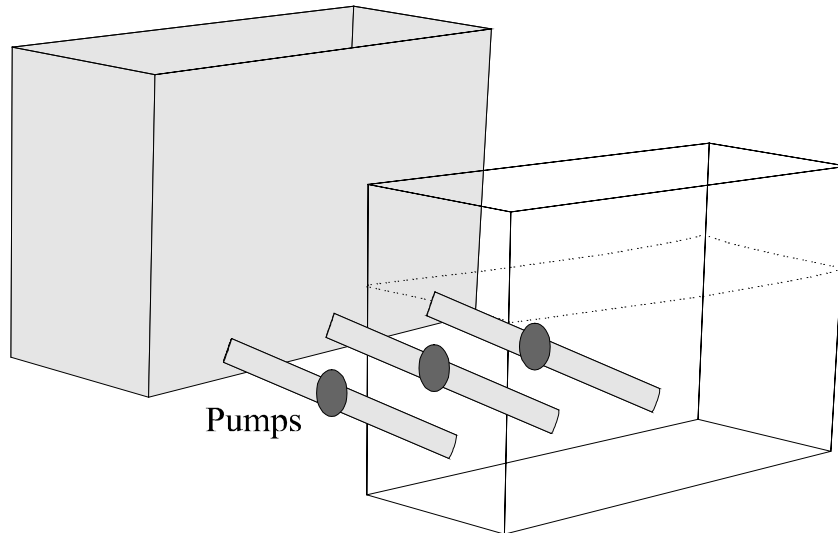


Figure 3-1. Anti-Roll Tank System

In Figure 3-1, the tanks shown are connected by pipes, which may or may not be outfitted with pumps. The pumps allow for the active control of the fluid motion, and the absence of the pumps allows the fluid to freely move in a passive system. For our purposes, the motion of this fluid is approximated by a point mass which either moves with a prescribed function of time (active system) or is free to oscillate (passive system).

3.2 Formulation of Active System in Reduced Model in LAMP

3.2.1 Theory and Assumptions

The motion of the liquid in the tanks is approximated by the motion of a point mass that moves from port to starboard. An initial formulation of this system is derived where the motion of the mass only influences the roll and sway degrees of freedom only. However, the formulation is based solely on the roll motion of the ship and no terms from the other ship degrees of freedom are used. This approximation is implemented to expedite testing the feasibility of including an active control system in the LAMP code and will hereafter be referred to as the two-degree-of-freedom model.

In Figure 3-2, a schematic of the moving mass is represented. The position of m as a function of time $d(t)$ is specified by a control law. The roll angle is specified by ϕ , and the roll velocity is specified by p .

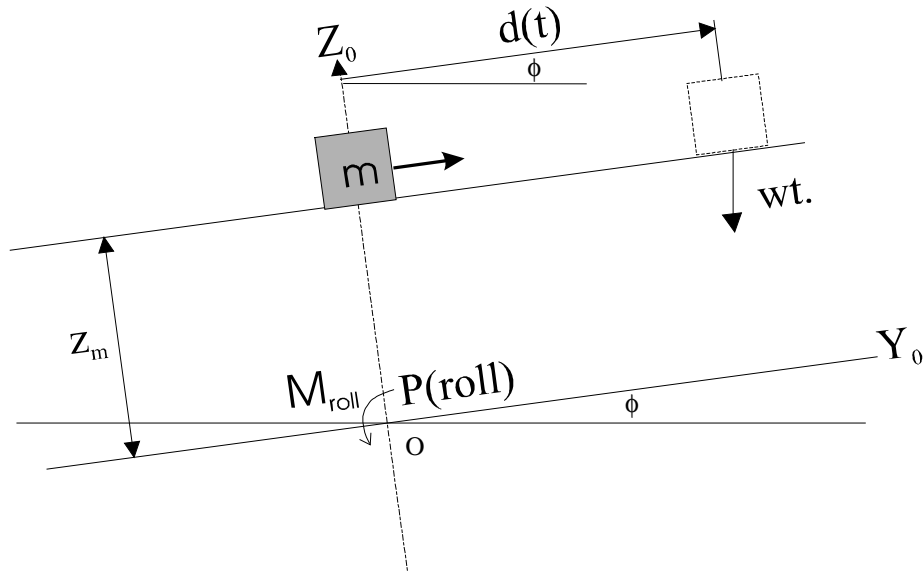


Figure 3-2. Initial Mass Motion Approximation

3.2.2 Mathematical Formulation

3.2.2.1 Forces Added to the Equations of Motion for the Ship

The mathematical model for the active system in two degrees of freedom is a straightforward application of Newton's law. The equations of motion for the ship in global coordinates are described by Fossen (1995) and are listed as follows:

$$[M]_{RB}^{6 \times 6} \dot{v} + [C]_{RB}^{6 \times 6} v = \tau_{RB} \quad [3.1]$$

where v is a vector of the velocities and derivatives of the Euler angles for all six degrees of freedom, and τ_{RB} is a vector of the forces.

The forces and moments that m exerts on the ship are added to the right hand side of the equations of motion:

$$[M]_{RB}^{6 \times 6} \dot{v} + [C]_{RB}^{6 \times 6} v = \tau_{RB} + F(t) \quad [3.2]$$

where $F(t) = \mathbf{A}[0, F_y, 0, M_x, 0, 0]^T$ and \mathbf{A} is the transformation matrix from the ship-fixed system to the global system. The force in sway is given by:

$$F_y = -m\ddot{d}(t) \cos(\phi) \quad [3.3]$$

The roll moment is generated by the forces from the weight of the mass, the force from the acceleration of the mass, and their respective distances from the center of gravity (Cg) of the ship as follows:

$$M_x = m\ddot{d}(t)z_m - mgd(t) \cos(\phi) \quad [3.4]$$

z_m is the height of the mass above the origin of the ship-fixed system, point O (see Figure 3-2.)

3.2.2.2 Servo Equation Specifying the Position of the Mass

Positioning of the mass m can be accomplished with the use of servomechanisms. The mass in this derivation is only free to move across the ship laterally and its lateral position is given by $d(t)$. The position for the mass is described by the following equation:

$$\ddot{d} + \mu\dot{d} + \omega^2(d - d_c) = 0 \quad [3.5]$$

where $d(t)$ is the actual position of the mass relative to a reference point fixed in the ship, d_c is the commanded position of the mass, μ and ω are constants which are chosen to achieve reasonable agreement between the actual servomechanism and the solution of this equation. Equation [3.5] describes how the mass responds to a specified command. It is solved using a Runge-Kutta fourth-order scheme at each time step; thus, another equation could be used in its place with no problem.

The commanded position of the mass, d_c , is specified by a simple PID controller:

$$d_c = G_1\phi + G_2 \int_{T-1}^T \phi dt + G_3 p \quad [3.6]$$

where ϕ is the roll angle of the ship. The values of G_1 and G_2 are set to zero in the present example. This means that the commanded position of the mass will produce a moment that always opposes the roll velocity of the ship. The physical effect of the active tank system is to add damping to the rolling motion.

Additional constraints were also imposed on the motion of the mass to ensure "physically reasonable" solutions. The size of the mass necessary to yield good control authority of a ship is approximately 1-2% of the displacement of the vessel, which is quite large. As such, the type of pump system necessary to move such a large volume of water must have some inherent limitations on acceleration and maximum velocity. Therefore, it was necessary to limit the maximum values for velocity and acceleration of the mass to more closely approximate the simulated motion of the fluid. The position of the mass also has a physical limit, which is the position of the actual tank. Typical values for the additional constraints placed on the solution of the mass motion are:

$$\ddot{d}_{\max} = 0.8g, \quad \dot{d}_{\max} = 13 \text{ ft/s}, \quad \text{and} \quad d_{\max} = 0.95B$$

where B is the half beam of the ship. The values for \ddot{d}_{\max} and \dot{d}_{\max} are chosen using a "reasonable guess" engineering approximation for the system physical limits while the value of d_{\max} represents the ship beam dimension limit.

The servo equation with the constraints described in this section is utilized in the active system simulation for the six-degree-of-freedom case discussed in the next section. As previously mentioned, the focus of this research is to show the efficacy of anti-roll tank systems in a time-domain simulation, not to develop sophisticated control algorithms. For this reason, the simple PID controller is used in all active-system simulations.

3.3 Formulation of the Active System for Six-Degree-of-Freedom Motion

3.3.1 System Theory and Assumptions

In this section, the full equations of motion of the active anti-roll tank system which influences all six degrees of freedom of the ship motion are presented. The amount of displaced fluid in the anti-roll tank system is approximated as a point mass which moves

from port to starboard and influences the ship motion in all six degrees of freedom. The position of the point mass is given as a function of its distance from the centerline, $d(t)$. Again, in this formulation there is no consideration given to the free surface of the tanks, and the motion of the mass is constrained to 95 percent of the half beam.

3.3.2 Mathematical Formulation

In order to derive the forces and moments that the moving mass, m , exerts on the ship in six-degree-of-freedom motion, it is necessary to derive the position, velocity, and acceleration terms of the ship relative to the ground-fixed coordinate system. The motion of m relative to the ship must then be described. It is convenient to use two coordinate systems: one fixed to the ship and the other fixed to the earth. The latter is considered an inertial system. The orientation of $\{X_o, Y_o, Z_o\}$ relative to the ground-fixed system $\{X, Y, Z\}$ is given by a set of Euler angles which completely characterize the orientation of the ship with respect to the ground-fixed coordinate system (see Fossen 1995).

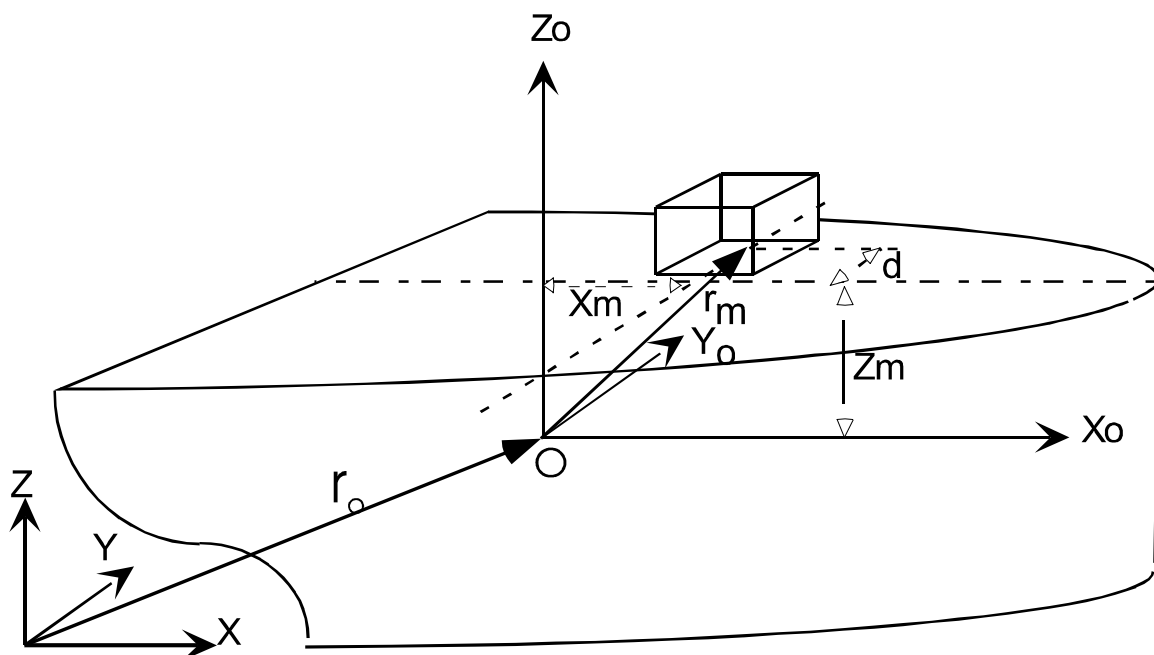


Figure 3-3. Coordinate System Diagram

In Figure 3-3, the vector $\mathbf{r}_o = \{x_o(t), y_o(t), z_o(t)\}$ represents the position in the inertial coordinate system of the origin of the ship-fixed coordinate system, \mathbf{O} . Vector $\mathbf{r}_m = \{x_m, d(t), z_m\}$ represents the position of the mass with respect to the body-fixed frame. The position of the mass in the global system is given by:

$$\mathbf{R}_m = \mathbf{r}_o + \mathbf{r}_m \quad [3.7]$$

The absolute velocity of point \mathbf{O} is given by $\mathbf{v}_o = \{u(t), v(t), w(t)\}$ where u , v , and w are the components along the ship-fixed system, and the components of the angular velocity of the ship are given by $\boldsymbol{\omega} = \{p(t), q(t), r(t)\}$ in the ship-fixed system. By taking the first derivative of \mathbf{R}_m with respect to time, we find the velocity of the mass in global coordinates to be:

$$\mathbf{V}_m = \mathbf{v}_o + \dot{\mathbf{r}}_m + \boldsymbol{\omega} \times \mathbf{r}_m \quad [3.8]$$

where $\dot{\mathbf{r}}_m$ is the velocity of m relative to the ship-fixed coordinate system. The acceleration of point \mathbf{O} is given by:

$$\mathbf{a}_0 = \dot{\mathbf{v}}_0 + \boldsymbol{\omega} \times \mathbf{v}_0 \quad [3.9]$$

where the components of \mathbf{a}_0 are referred to the ship-fixed coordinate system. By taking the first derivative of \mathbf{V}_m and $\boldsymbol{\alpha} = \{\dot{p}(t), \dot{q}(t), \dot{r}(t)\}$ where $\boldsymbol{\alpha}$ is the angular acceleration, we find the acceleration of the mass in global coordinates to be:

$$\mathbf{A}_m = \mathbf{a}_0 + \ddot{\mathbf{r}}_m + \boldsymbol{\omega} \times \dot{\mathbf{r}}_m + \boldsymbol{\alpha} \times \mathbf{r}_m + \boldsymbol{\omega} \times (\dot{\mathbf{r}}_m + \boldsymbol{\omega} \times \mathbf{r}_m) \quad [3.10]$$

The force exerted on the mass by the ship and gravity is

$$\mathbf{F}_m = -m\mathbf{g} + m\mathbf{A}_m \quad [3.11]$$

where $\mathbf{g} = \{g_x, g_y, g_z\}$ is the acceleration vector due to gravity in the ship-fixed coordinate system. The force exerted on the ship by the mass is given by:

$$\begin{aligned} \mathbf{F}_s &\equiv -\mathbf{F}_m \\ &= m\mathbf{g} - m\mathbf{A}_m \\ &= m(g_x - \ddot{u} - gw + rv + 2r\dot{d} - \dot{q}z_m + \dot{r}d - qpd + q^2x_m - rpz_m)\hat{i} + \\ &\quad m(g_y - \dot{v} - ru + pw - \ddot{d} - \dot{r}x_m + \dot{p}z_m - rpz_m + r^2d + p^2d - pqx_m)\hat{j} + \\ &\quad m(g_z - \dot{w} - pv + qu - 2p\dot{d} - \dot{p}d + \dot{q}x_m - rpx_m + p^2z_m + q^2z_m - rqd)\hat{k} \end{aligned} \quad [3.12]$$

The moment of \mathbf{F}_s about a point \mathbf{O} in the ship is given by:

$$\begin{aligned} \mathbf{M}_0 &= \mathbf{r}_m \times \mathbf{F}_s \\ &= m[z_m(g_y - \dot{v} - ru + pw - \ddot{d} - \dot{r}x_m + \dot{p}z_m - rpz_m + r^2d + p^2d - pqx_m) \\ &\quad - d(g_z - \dot{w} - pv + qu - 2p\dot{d} - \dot{p}d + \dot{q}x_m - rpx_m + p^2z_m + q^2z_m - rqd)]\hat{i} \\ &+ m[x_m(g_z - \dot{w} - pv + qu - 2p\dot{d} - \dot{p}d + \dot{q}x_m - rpx_m + p^2z_m + q^2z_m - rqd) \\ &\quad - z_m(g_x - \dot{u} - gw + rv + 2r\dot{d} - \dot{q}z_m + \dot{r}d - qpd + q^2x_m - rpz_m)]\hat{j} \\ &+ m[d(g_x - \dot{u} - gw + rv + 2r\dot{d} - \dot{q}z_m + \dot{r}d - qpd + q^2x_m - rpz_m) \\ &\quad - x_m(g_y - \dot{v} - ru + pw - \ddot{d} - \dot{r}x_m + \dot{p}z_m - rpz_m + r^2d + p^2d - pqx_m)]\hat{k} \end{aligned} \quad [3.13]$$

The forces and moments listed in [3.12] and [3.13] are substituted for \mathbf{F} in the equations of motion [3.2]. The position of the mass is given by the servo equation with the same constraints as discussed in section 3.2.2.2.

3.4 Formulation of Passive Anti-Roll Tank System in Six Degrees of Freedom

3.4.1 Theory and Assumptions

In this section, the equations of motion are formulated for the passive anti-roll tank system, which influences all six degrees of freedom of the ship motion. Again the amount of displaced fluid in the anti-roll tank system is approximated as a point mass that freely moves from side to side and influences the ship motion in all six degrees of freedom. As with the active tank system, the motion of the mass is strictly from port to starboard and the position of the mass is given as a function of time by $d(t)$. However, in this formulation, the mass moves from port to starboard as if attached to the ship like a spring-mass-damper instead of having a control algorithm to specify a desired position. The only restrictions on the motion are specified maximums for position, velocity, and acceleration. These maxima

are physical constraints that are adjusted to provide a reasonable approximation to the freely moving fluid in the tanks.

3.4.2 Mathematical Formulation

The derivation for the position, velocity and acceleration of the mass in the passive tank formulation is performed the same way as shown in section 3.3.2. The coordinate systems used to describe the position of the mass are the same as those shown in Figure 3-3, and the forces and moments exerted on the ship by the moving mass are still given by equations [3.12] and [3.13].

However, the motion for the mass is specified by a different differential equation than the servo equation listed for the active tank formulation. This formulation is borrowed from standard vibration-absorption theory as described in den Hartog [1985]. The premise being that there is an additional degree of freedom, which corresponds to the free motion of another mass. This second mass system is tuned in such a way as to absorb the energy near or at resonance from the primary system. In essence, the smaller mass system (i.e. tank system) moves a great deal while the primary system (i.e. the ship) moves less.

The standard equation for the mass motion is given by:

$$\ddot{d} + \mu_m \dot{d} + \omega_m^2 d = 0 \quad [3.14]$$

where d is the position, μ_m the damping constant, and ω_m is the system natural frequency. But this differential equation does not account for the additional accelerations, which couple the mass to the ship. These terms are found by taking the Y component of equation [3.12], dividing by m to obtain the acceleration, and removing all of the coupling and non-linear terms. Once these additional terms are added, we find the equation of motion for m to be:

$$\ddot{d} + \mu_m \dot{d} + \omega_m^2 d - g_y + z_m \dot{p} = 0 \quad [3.15]$$

Equation [3.15] will be solved by a Runge-Kutta fourth-order method. The spring and damping constants correspond to geometric relations of the actual physical tank system. Since we are approximating the actual tank system as a moving mass, the methodology for converting the spring and damping terms into terms that correlate with the physical dimensions of a real tank system are only mentioned here. One source for the details of tank sizing and placement is the Design Data Sheet (DDS) # 565-1 published by the US Navy.

Chapter 4 Single-Degree-of-Freedom Simulator (MOTSIM)

4.1 Motivation for Simulator, Theory, and Assumptions

A single-degree-of-freedom computer simulator is developed to approximate the ship motions in the roll degree of freedom. This simulator, called MOTSIM, is tuned (see section 5.2.1) to nearly match the roll motions predicted by LAMP and runs many times faster than LAMP. The reduced simulation time allows for the study of numerous long runs in which steady-state motion may be obtained. The goal was to use MOTSIM as a test bed for the active and passive control strategies, system mathematical formulations, and for studies of the influences of the various parameters. After the control systems have been somewhat optimized in MOTSIM, they are implemented as subroutines in the LAMP program.

The basis of MOTSIM is a single equation for the ship roll motion. The motion of the mass is specified by an additional equation of motion.

4.2 MOTSIM Mathematical Formulation

4.2.1 Approximation for Ship Roll Equation of Motion

The mathematical formulation for the roll equation of motion used in MOTSIM is very straightforward. It follows from equation [3.13] that the moment about the x-axis (roll) that the mass exerts on the ship is given by:

$$M_x = m[z_m(g_y - \dot{v} - ru + pw - \ddot{d} - \dot{r}x_m + \dot{p}z_m - rpz_m + r^2d + p^2d - pqx_m) - d(g_z - \dot{w} - pv + qu - 2p\dot{d} - \dot{p}d + \dot{q}x_m - rpx_m + p^2z_m + q^2z_m - rqd)].$$

In addition to this moment, there is a hydrodynamic moment, which includes damping and restoring components and a forcing function that approximates the action of the waves, that must be added to the right hand side of the equation as follows:

$$I_{xx}\dot{p} + \mu_s p + k_s \phi = m[z_m(g_y - \dot{v} - ru + pw - \ddot{d} - \dot{r}x_m + \dot{p}z_m - rpz_m + r^2d + p^2d - pqx_m) - d(g_z - \dot{w} - pv + qu - 2p\dot{d} - \dot{p}d + \dot{q}x_m - rpx_m + p^2z_m + q^2z_m - rqd)] + F_w \cos(\Omega t)$$

where μ_s is the hydrodynamic damping coefficient, k_s is the coefficient for the hydrodynamic restoring force, F_w is the amplitude of the wave induced moment, and Ω is the encounter frequency. When the motion is restricted to a single degree of freedom in roll and the cubic non-linear terms are assumed to be small and removed from this equation, we find:

$$I_{xx}\dot{p} + \mu_s p + k_s \phi = m[z_m(g_y - \ddot{d} + \dot{p}z_m) - d(g_z - 2p\dot{d} - \dot{p}d - z_m p^2)] + F_w \cos(\Omega t)$$

By substituting constant $k_s = I_{xx}\omega_s^2$, where ω_s is the natural frequency in roll and solving for \dot{p} , we obtain the equation for the roll acceleration of the ship with the influence of the mass position, velocity, and acceleration in tact:

$$\dot{p} = \frac{1}{I_{xx} - md^2 - mz_m^2} \left[-\omega_s^2 I_{xx} \phi - \mu_s p + m(z_m g_y - z_m \ddot{d} + z_m p^2 d - d g_z + 2p d \dot{d}) \right] + F_w \cos(\Omega t) \quad [4.1]$$

The procedure for numerically solving this equation is discussed in detail in section 4.2.3.

4.2.2 Active and Passive System Motion

The MOTSIM program can include an active mass motion system or a passive “vibration absorber” system. The mathematical formulation for the active mass motion is exactly the same as presented in Section 3.2.2 in equation [3.5] where the equation of motion for the mass is specified by the servo equation

$$\ddot{d} + \mu\dot{d} + \omega^2(d - d_c) = 0$$

which is tuned in the same manner previously discussed. The PID control law found in equation [3.6] and repeated here determines the commanded position of the mass.

$$d_c = G_1\phi + G_2 \int_{T-1}^T \phi dt + G_3 p$$

As mentioned in the earlier discussion of these equations, G_1 and G_2 are set to zero. The MOTSIM program, because of its inherent simplicity, allows us to find G_3 by a classical control theory approach that is discussed in section 5.2.2.1.

The mathematical formulation for the passive system is very much the same as described in section 3.4.2 where the equation of motion for the mass is given by [3.15] and repeated here.

$$\ddot{d} + \mu_m\dot{d} + \omega_m^2 d - g_y + z_m\dot{p} = 0$$

4.2.3 Solution Technique

The solution technique used in the MOTSIM program must solve the equations of motion for both the ship and the mass simultaneously. This is a necessary requirement because we have acceleration terms for both the mass and the ship in each differential equation. A modified form of the Hamming fourth-order predictor-corrector technique was used. The Hamming method iterates at each time step until the difference between two successive iterations drops below some specified tolerance. The iteration process allows us to use values for the solution of each acceleration term at the previous iteration in the current iteration. The method also requires no knowledge of the added mass, nor does it require the calculation of the added mass. The Hamming method is described in detail in *Applied Numerical Methods* [1969].

Chapter 5 Results

5.1 Ship Type and Configuration Used in Analysis of Tank Systems

As previously mentioned the operational regime for ships fitted with anti-roll tanks is in the slow to medium speed range. The Series 60, $C_B = 0.7$ cargo ship was selected for evaluating the active and passive tank system in LAMP. Series 60 ships have a common hull form that has been in service for many years. Table 5-1 outlines the specifications of this specific hull-form, and the hull form geometry is represented in Figure 5-1. The ship is specified with 300 panels for the LAMP computations, and a non-dimensional time step of 0.04 is used. These values for panelization and time step provide convergence to experimental data for the ship motion simulation.

Table 5-1. Series 60, $C_B = 0.7$ Parameters and Specifications

| | | |
|---------------------|---|--------------------------|
| LBP | = | 400 ft. |
| Beam | = | 57.14 ft. |
| Draft | = | 22.86 ft. |
| C_B | = | 0.7 |
| Displacement | = | 10,460 LSW |
| Freeboard Amidships | = | 10 ft. |
| VCG | = | 20.79 ft. above baseline |

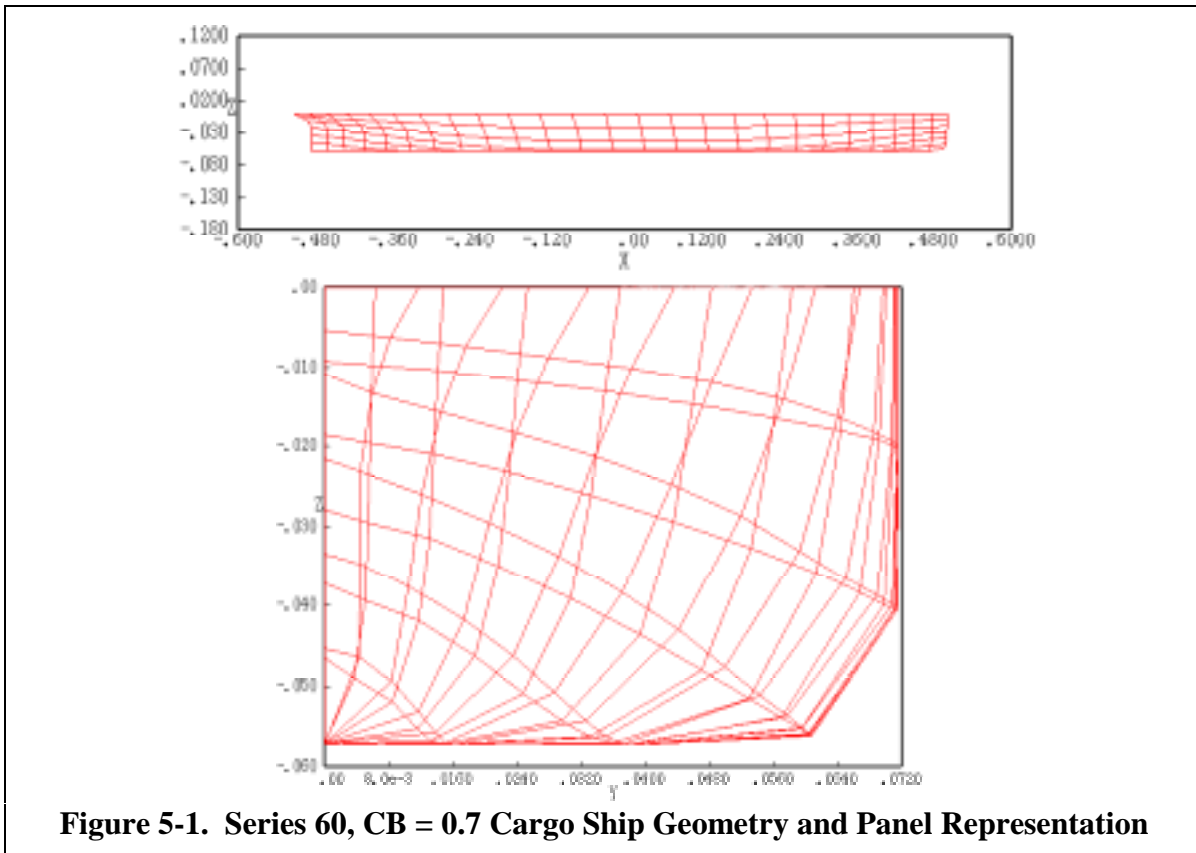


Figure 5-1. Series 60, $C_B = 0.7$ Cargo Ship Geometry and Panel Representation

The LAMP program was configured to run in the LAMP-2 mode as described in section 2.1. LAMP has a very extensive set of variables that are defined in an input data file. The data set the configuration and various options. The cases of forced motion considered in this research correspond to a beam seaway with a single sinusoidal wave. The wave height (and frequency are adjusted to give waves in the linear regime with an amplitude-to-wavelength ratio of less than 1/50. The non-dimensional values for the wave frequency and amplitude are 2.0 and 0.04 respectively, where the frequency is non-dimensionalized by $\sqrt{g/L}$ and the amplitude is by L . The cases of initial roll displacement are run in a calm water seaway. A sample of one of the input files used in a beam sea case is shown in Appendix A.

The settings used in the evaluation of the MOTSIM program correspond to the values found in the Series 60, CB = 0.7 hull form. The mass, moment of inertia and other necessary quantities from the Series 60, CB = 0.7 are used to tune the system used in the MOTSIM program, so that the roll motion predicted by MOTSIM is to have the same dynamic behavior of the same ship in the LAMP program. The tuning method is discussed in section 5.2.1.

5.2 Theory and System Study Using MOTSIM

The MOTSIM program is used to evaluate the system configuration, approximations, and the control-system strategy before the full implementation is installed in one of the LAMP programs as described in Chapter 4. MOTSIM is also used to evaluate the influence of several nonlinear terms used in the mathematical models described in section 4.2. The following sections discuss the tuning of MOTSIM to the LAMP model; the techniques used in the evaluation of the models, and the results obtained from the active and passive system implementations.

5.2.1 Tuning MOTSIM to Match the LAMP Simulation

In order to ensure that the roll motion characteristics predicted in the MOTSIM model are similar to those predicted in the LAMP model, several coefficients in MOTSIM are tuned so that the motion history of two distinct cases matched the history of a LAMP simulation. The two cases used are an initial displacement case and a forced beam sea case. From the equation of motion [4.1], the value of μ_s is adjusted by using the initial displacement case such that MOTSIM yields the same damping characteristics seen in the LAMP model. Likewise, F_w is adjusted by using the forced beam sea case so that the steady-state amplitude of the motion predicted in LAMP and MOTSIM are approximately equal.

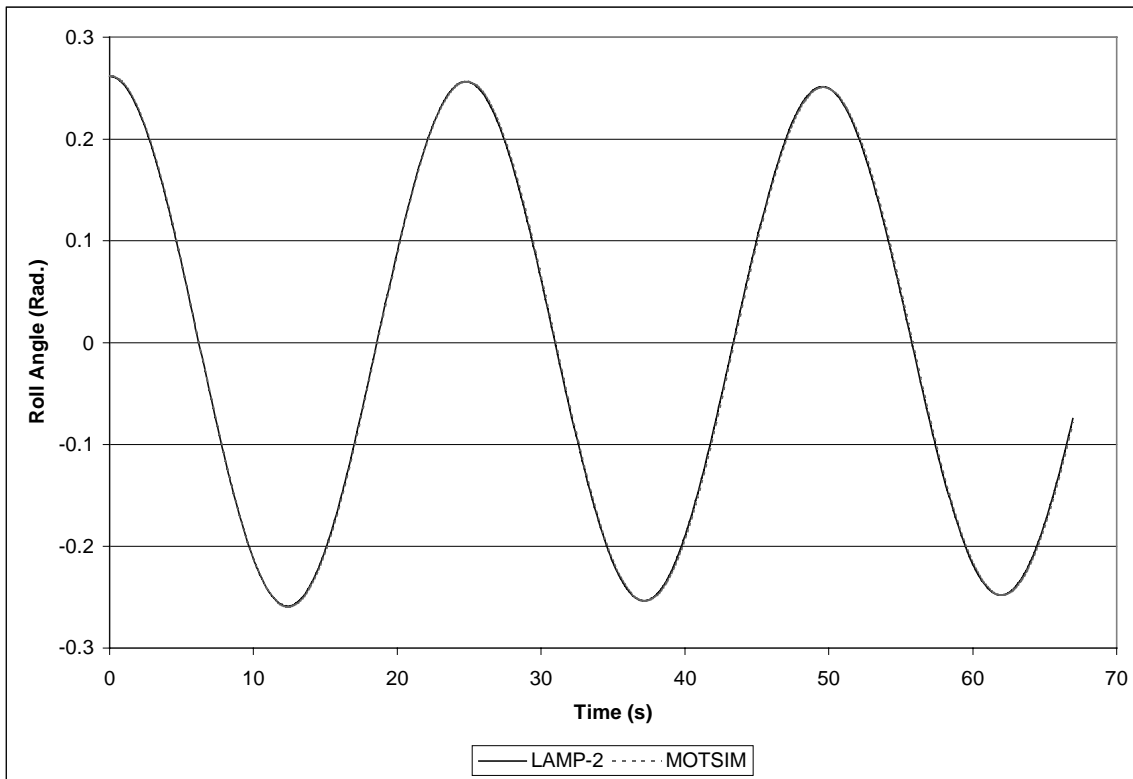


Figure 5-2. Motion History of Initial Displacement Case in Calm Water Used to Tune MOTSIM to LAMP

In Figure 5-2, the result of tuning the damping coefficient μ_s is shown, where μ_s is varied until the following condition on the logarithmic decrement is satisfied:

$$\log \left[\frac{amp_1}{amp_2} \right]_{LAMP} = \log \left[\frac{amp_1}{amp_2} \right]_{MOTSIM} \quad [4.2]$$

The values of amp_1 and amp_2 correspond to the first and second successive amplitudes of the relative simulation history. A non-dimensional value of $\mu_s = 2.56 \times 10^{-6}$ yields a very accurate correlation between the LAMP-2 simulation and the MOTSIM simulation as seen in motion histories presented in Figure 5-2. The matching of the coefficients and damping terms in MOTSIM to the damping modeled in LAMP may be modified in future versions. As the roll-damping model used in LAMP is improved, it may become necessary to include nonlinear damping coefficients as well. However at present, the linear coefficient provides an excellent approximation to the damping computed in LAMP.

Tuning the forcing-function amplitude F_w used in MOTSIM to the motion in LAMP is not as critical as tuning the damping model, because in MOTSIM the forcing function is used to cause the motion of the system to reach a desired steady-state amplitude. In LAMP, the wave amplitude also causes the motion to reach a steady-state amplitude, but the actual forces calculated are very different from the simple forcing used in MOTSIM. We cannot hope to exactly match the time history predicted by the LAMP model unless we find a more complicated forcing function that more accurately approximate the pressure forces modeled in LAMP. The LAMP formulation includes a memory term in the form of a convolution integral (see section 2.2 on LAMP mathematical formulation). There is also coupling with the other degrees of freedom that extends well beyond the scope of the MOTSIM model.

The forcing function used in MOTSIM is fairly simple since we are only concerned with the validation of the control system, the percent reduction in roll motion, and methodology of the anti-roll tank approximations. The actual time history itself is not of significant importance in this work, and thus only the steady-state amplitude of the MOTSIM and LAMP models is of importance.

5.2.2 Active-System Implementation

The results from the active-system implementation in MOTSIM are presented in this section. The approach used for determining the gain for the PID control system, the results from a sample initial displacement case and the results from a sample forced motion case are presented. The active system implemented in MOTSIM is formulated in section 4.2.2.

5.2.2.1 Classic Approach for Controller Coefficient

As previously mentioned, a classical control theory approach was used in obtaining the value for the G_3 gain from equation [3.6]. Specifically, a root locus technique was applied to a simplified system model as represented in the block diagram shown in Figure 5-3. The information presented in this section was meant to be an overview of the technique used in the commercially available program MATLAB® to find the G_3 gain. For more information on the root locus technique as applied in MATLAB®, please consult a control system design text such as Shahian & Hassul [1993].

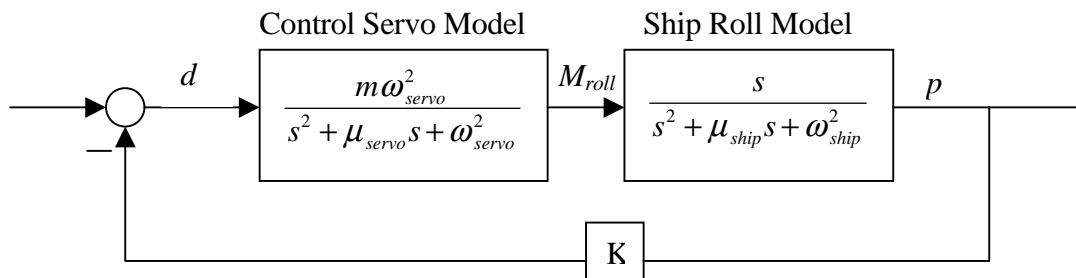


Figure 5-3. System Block Diagram

The block diagram in Figure 5-3 shows the Laplace transforms for the second order equations of the servo model and the roll degree of freedom model. The inputs and outputs of the blocks are d , M_{roll} , and p where d is the mass position, M_{roll} is the roll moment the mass motion generates, p is the roll velocity resulting from the ship equation of motion. The K block equates to the G_3 gain from equation [3.6]. The *rlocus* utility in MATLAB® was used to generate the root locus plot for this system and the *rlocfind* utility was used to arbitrarily select a gain that provided a left-hand-plane or stable solution. The required parameters for the *rlocus* utility are the numerator and denominator of the open loop system.

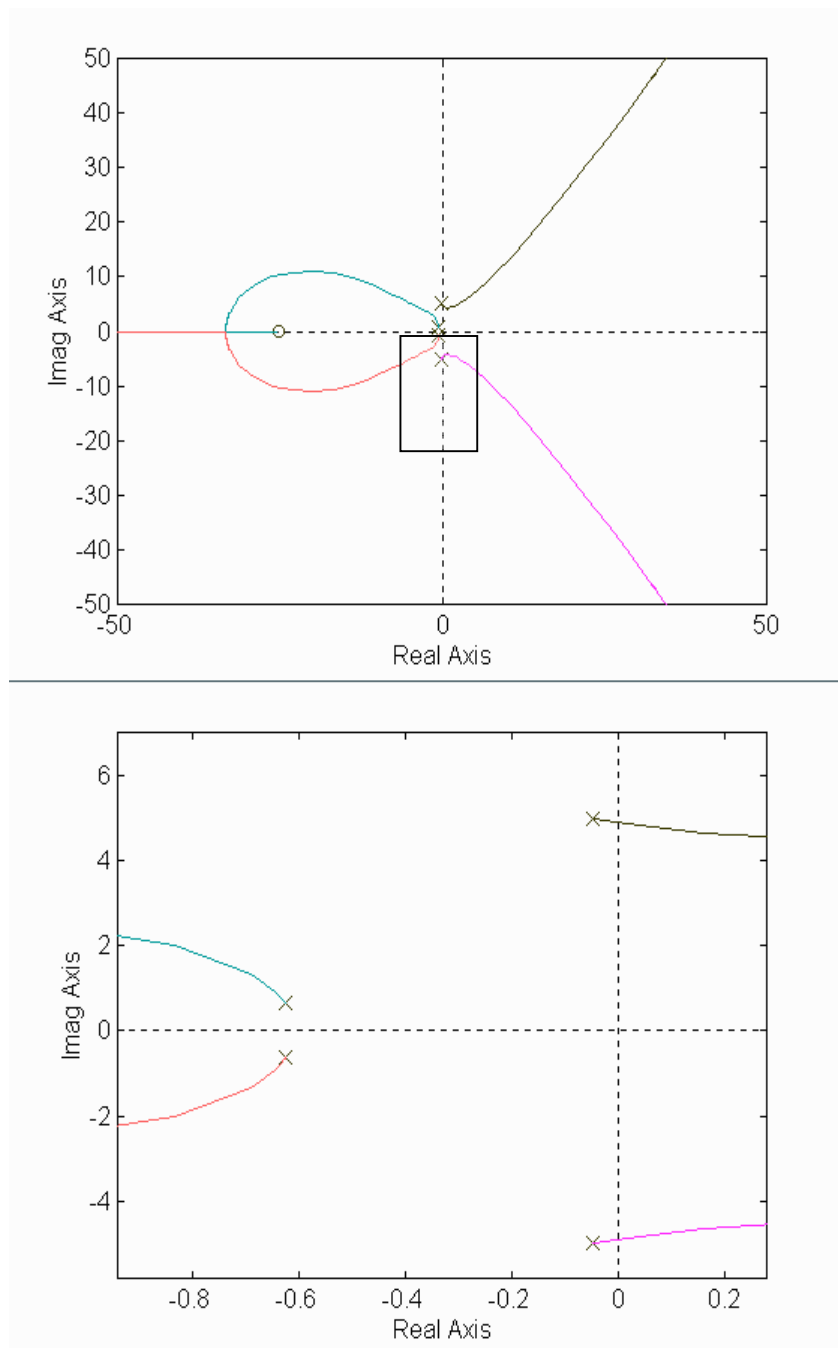


Figure 5-4. System Root Locus and Zoomed Region

In Figure 5-4, the root locus plot for the simplified system is shown with a zoomed view of the pole region of interest. The controller gain G_3 is chosen so that it corresponds to pole values in the left or negative real plane. The result of this root-locus process is a G_3 value of 1.2. This value is used in the active control systems for both the MOTSIM and LAMP results.

5.2.2.2 Initial Displacement Case

For the first case in MOTSIM, the system is given an initial displacement of 16 degrees of roll and allowed to oscillate. The active controller then attempts to reduce the amplitude of the roll motion as described in section 4.2.2. In Figure 5-5, a comparison of the roll motion history of an initial-displacement case with no control and a case where the

moving mass (m) is equal to 2% of the total ship mass (M_{ship}) are shown. The position (d) and the commanded position (d_c) of the mass are also shown on this plot.

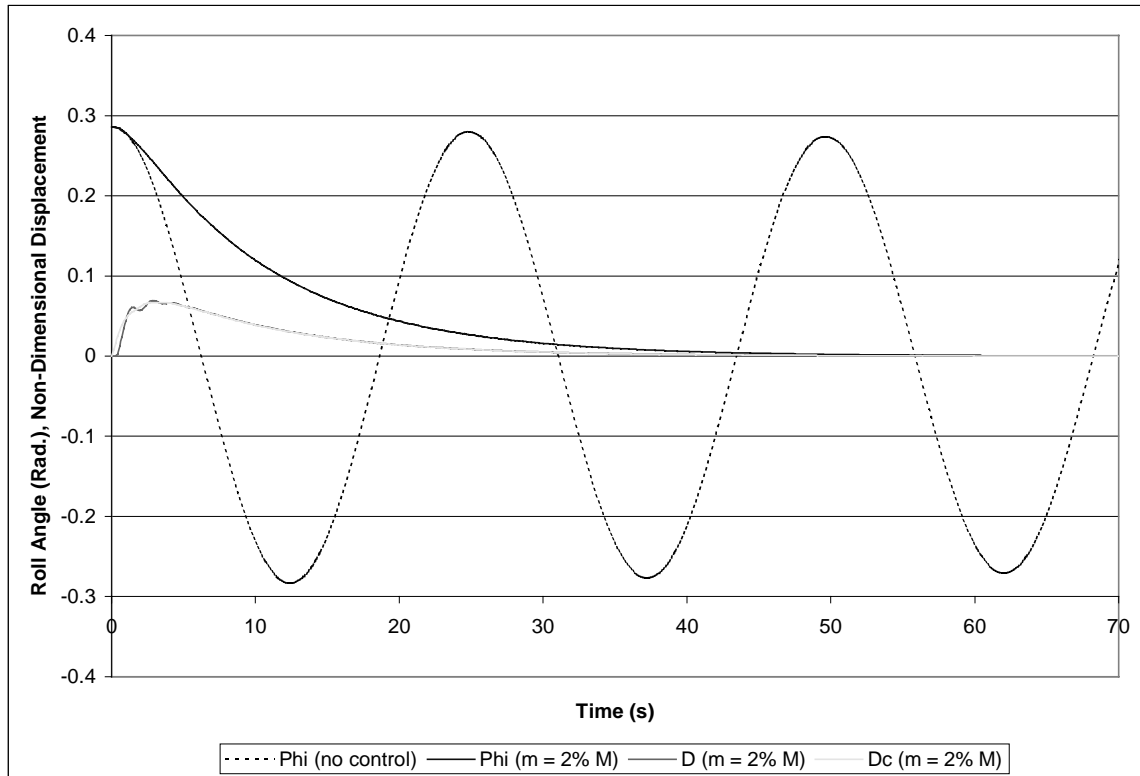


Figure 5-5. Motion History Following Release from an Initial Displacement for Two Cases: a) Ship Without Control b) Ship with Active Control where $m = 2\% M_{ship}$

The results in Figure 5-5 show that the roll motion of the ship may be damped out by using an active system where the commanded position of the mass is proportional to only the roll velocity of the system as described in section 3.2.2.2. They also show that sufficient control authority may be generated when m is 2% of M_{ship} .

5.2.2.3 Motion with Sinusoidal Forcing Function

In this section a forced-motion case is presented to show that the active control system reduced the amplitude of the roll motion when a sinusoidal forcing function is present. This case is representative a ship being forced by waves. The forcing function is of the form $f_w \cos(\Omega t)$ as shown in [4.1] where the non-dimensional values for the forcing amplitude f_w and the encounter frequency Ω are $1.0e-7$ and 0.8925 , respectively. The encounter frequency is also nearly equal to the ship's natural frequency in roll, a condition that produces the largest steady-state amplitudes. Figure 5-6 shows that when no control is applied to the system, a steady-state amplitude of 0.43 radians (25 degrees) is obtained.

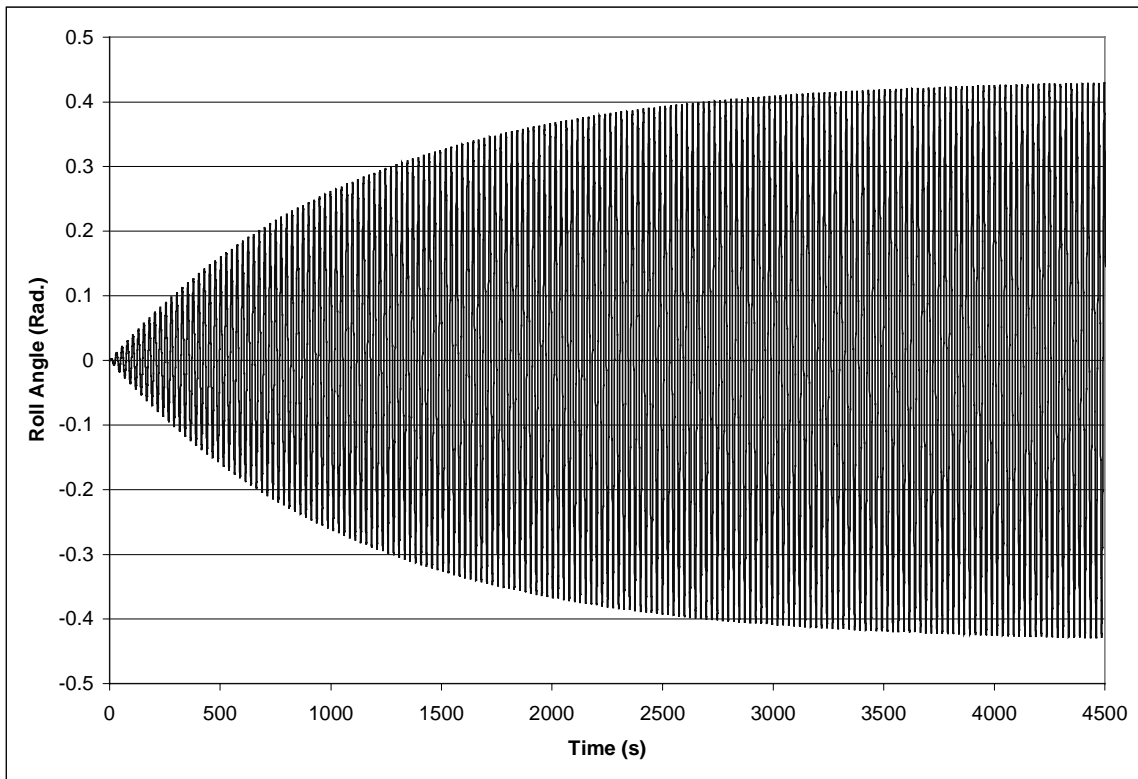


Figure 5-6. History of the Wave-Excited Motion for a Ship without Roll Control

The response is quite different for the actively controlled system with the same forcing function previously mentioned and the G_3 value found in section 5.2.2.1. The steady-state amplitude of the system is reduced to 1.1×10^{-3} radians (0.06 degrees), which equates to a 99% reduction, as shown in Figure 5-7. The amplitude reduction seen in Figure 5-7 confirms that the active system with m equivalent to 2% of M_{ship} yields very favorable, although probably somewhat optimistic, motion characteristics. The results must be considered optimistic since the roll-damping model used in the LAMP code may under-predict the actual roll damping seen by the ship.

Figure 5-8 shows a reduced time history for wave-excited motion so that the mass position (d) and the commanded mass position (d_c) may be seen on the same plot with the roll amplitude. It may be seen that the position of m lags the roll motion angle ϕ . This phase lag results in the additional damping that the controller adds to the system.

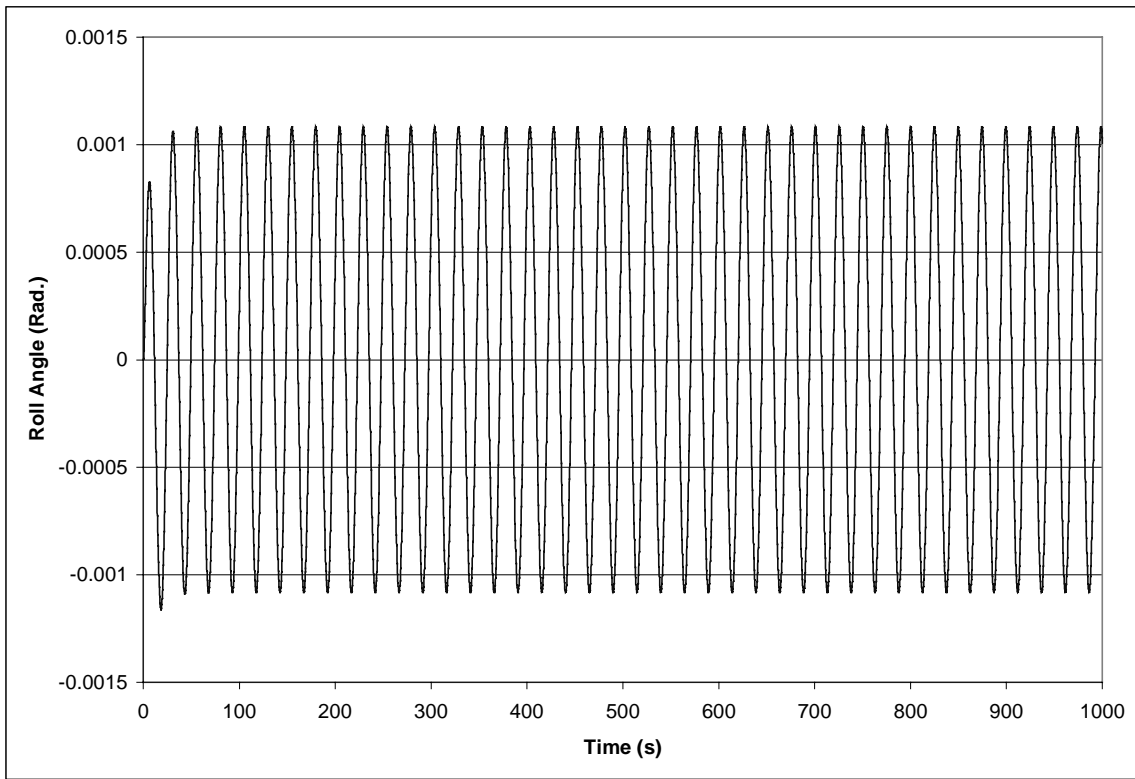


Figure 5-7. History of the Wave-Excited Motion for a Ship with an Active Control System where $m = 2\% M_{ship}$

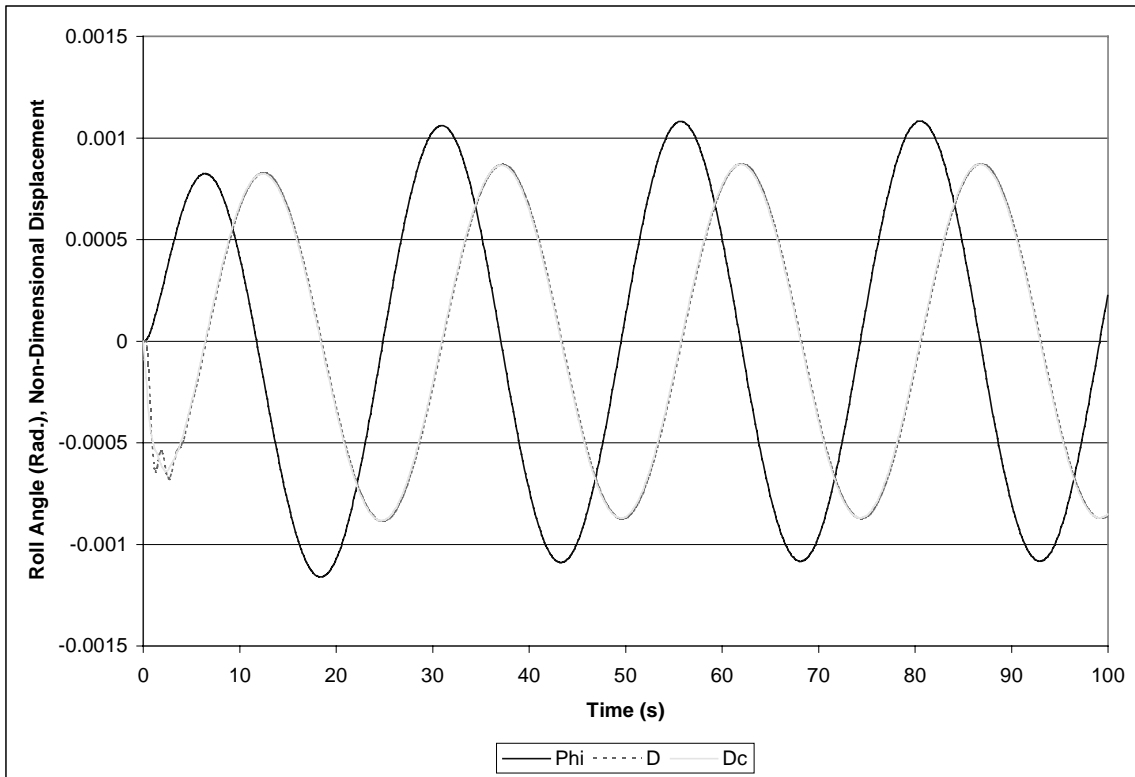


Figure 5-8. Reduced Time History for a Wave-Excited Motion of a Ship with an Active Control System where $m = 2\% M_{ship}$

5.2.3 Passive System Implementation

The results from the passive system implementation in MOTSIM are presented in this section for a sample initial-displacement case and a sample forced-motion case. The passive system implemented in MOTSIM is formulated in section 4.2.2. The ω_m and μ_m values from the mass system equation of motion [3.15] are set to the ship natural frequency ω_{ship} and 10% ω_{ship} , respectively, for both the case with initial-displacement and the case with the sinusoidal forced motion.

5.2.3.1 Initial Displacement Case

For the first case of the passive system in MOTSIM, the system was given an initial displacement equivalent to 16 degrees of roll and allowed to oscillate. The passive system acts as a vibration absorber that has the effect of reducing the amplitude of the roll motion as described in section 4.2.2.

Figure 5-9 shows a comparison of the roll motion history of a case with no control and a case where the moving mass (m) is equal to 2% of the total ship mass (M_{ship}). In this case d is initially non-zero. The position of the mass, d , is also shown in this figure.

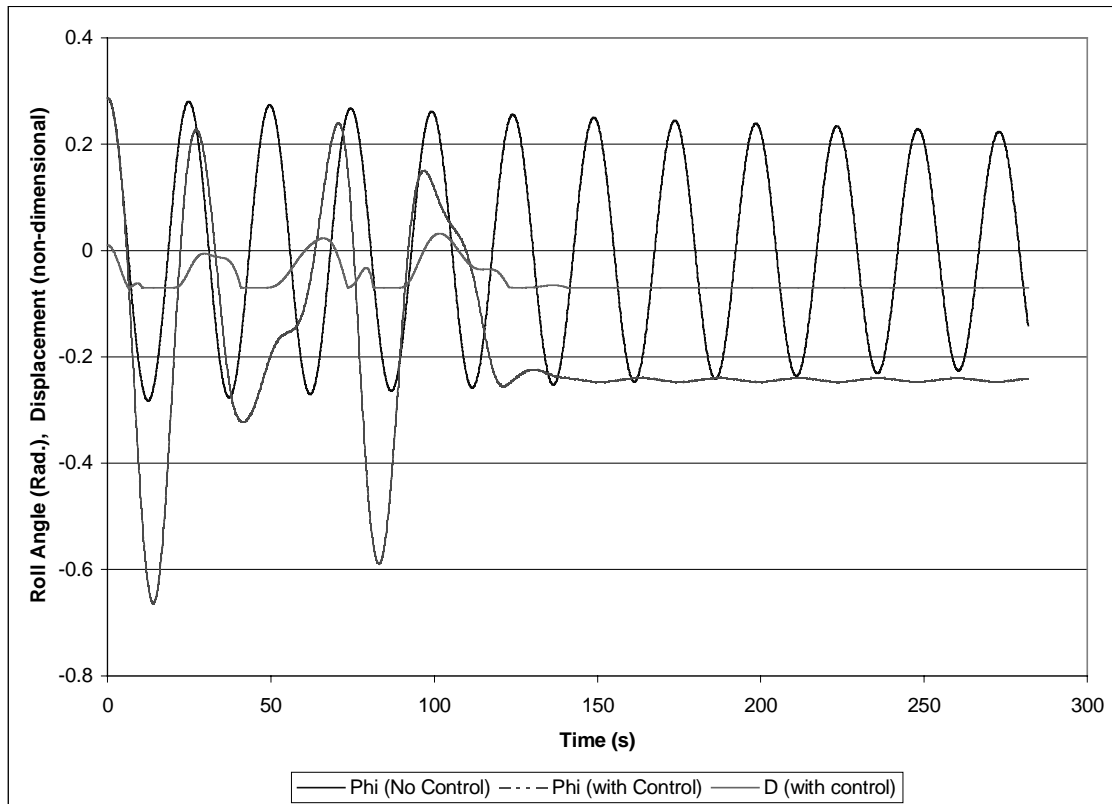


Figure 5-9. Roll Histories Following an Initial Displacement and No Wave Excitation for Two MOTSIM Cases: a) Case without Control b) Case with Passive Control Where $m = 2\% M_{ship}$

The history presented in Figure 5-9 shows that the passive system does not seem to work very well for the initial displacement case. The system does damp out the amplitude of the roll motion, but the resulting equilibrium position is a nonzero value. In the data

presented for the active system, the position of m was controlled and produced a steady-state amplitude of zero. In the active system, the roll velocity went to zero, but the roll amplitude could still have settled to a nonzero final value. The passive system has no active mechanism so as the oscillations of the roll motion damp out the controller loses its effectiveness. The resulting non-zero roll amplitude may also suggest that there are countless stable solutions for the initial displacement case, because for every possible position of the mass there exists a roll angle which produces a moment equilibrium.

5.2.3.2 Motion with Sinusoidal Forcing Function

The forced motion case presented in this section is the same case shown in section 5.2.2.3 for the active controller. The performance of the passive control system was evaluated when a sinusoidal forcing function is present. The forcing function is of the form $f_w \cos(\Omega t)$ as shown in [4.1] where the non-dimensional values for the amplitude f_w and the encounter frequency Ω are $1.0e-7$ and 0.8925 , respectively. The encounter frequency is nearly equal to the ship's natural frequency in roll, a condition that produces the largest steady-state amplitudes.

The steady-state roll amplitude from the forced motion case with no control present was previously shown in Figure 5-6. The forcing function caused the system to reach a steady-state roll amplitude of 0.43 radians (25 degrees).

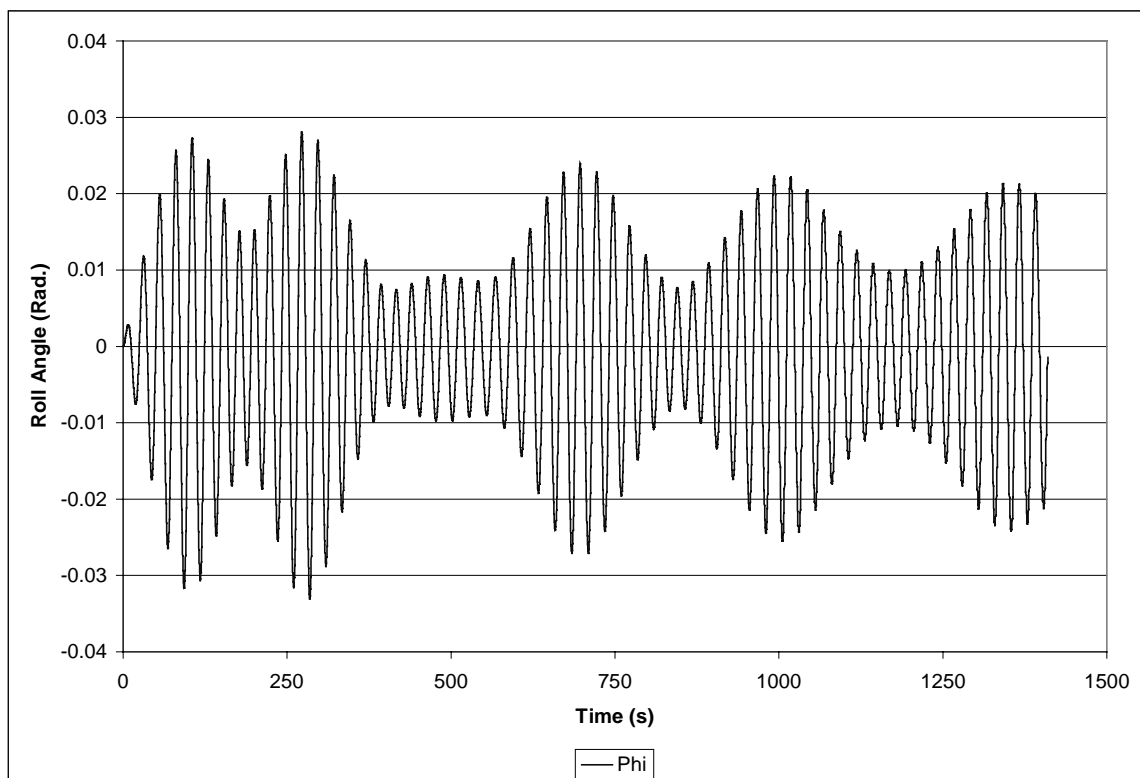


Figure 5-10. History of the Wave-Excited Motion of a Ship with a Passive-Control System where $m = 2\% M_{ship}$

In Figure 5-10, the response of the passive system is represented for the forced motion case when $m = 2\% M_{ship}$. The system has not quite reached a steady-state value for the time

history shown, but the amplitude of the roll angle has been reduced from 0.43 radians for the no control case to approximately 0.02 radians (1.15 degrees) or a 95% reduction. The passive system is very effective in absorbing the energy from the forcing function, and therefore the ship roll motion is reduced.

In Figure 5-11, a reduced time history is represented for the same forced motion case. The position of the mass is also shown. This figure shows that the position of m is always out of phase with the roll motion. The phase lag, which at times is 180° , is what is responsible for reducing the motion. The position of m never exceeds a non-dimensional value of 0.0015, which corresponds to only 2% of the ship half-beam. This indicates that the shipboard system can be confined to a relatively small space. A more complete investigation into the distance that the mass can move is conducted in section 5.2.4.

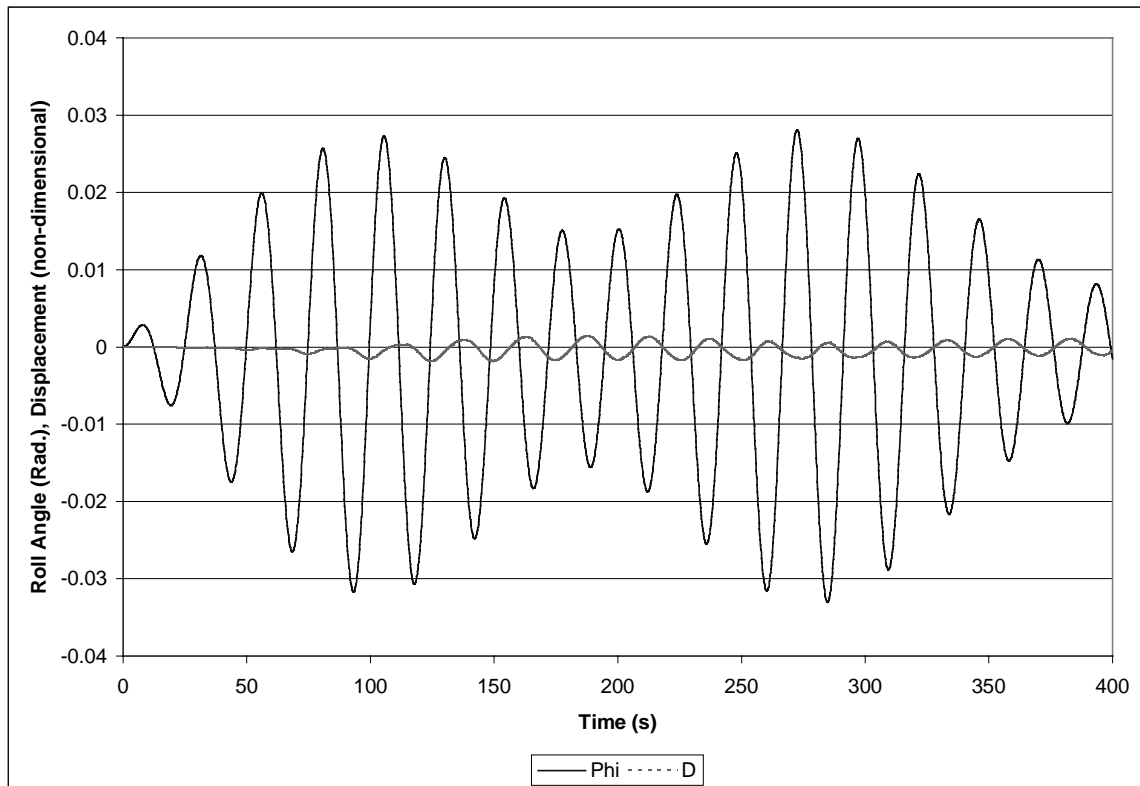


Figure 5-11. Reduced Time History for Wave-Excited Motion of a Ship with a Passive-Control System where $m = 2\% M_{ship}$

5.2.4 Coefficient Influence Study

A study is performed to find the influence on the motion of several of the terms used in the MOTSIM formulation. The equation for the roll acceleration, equation [4.1], is derived in section 4.2.1 and is re-written here.

$$\dot{p} = \frac{1}{I_{xx} - md^2 - mz_m^2} \left[-\omega_s^2 I_{xx} \phi - \mu_s p + m(z_m g_y - z_m \ddot{d} + z_m p^2 d - dg_z + 2p d \dot{d}) \right] + F_w \cos(\Omega t)$$

The active and passive system implementations are used to perform an investigation that consisted of the variation of system parameters such as m , z_m , and d_{max} . The following

investigations are performed with the same forcing function as described in section 5.2.2.3 where the non-dimensional values of f_w and Ω are $1.0e-7$ and 0.8925 , respectively.

Perhaps the most critical quantity on the overall feasibility of a shipboard anti-roll tank system is the amount of mass necessary to achieve reasonable control authority. In the initial part of the study the value of m is varied. In Figure 5-12, the steady-state roll amplitude is shown as a function of m .

In Figure 5-12, the steady-state roll motion is greatly influenced by m . Even the case where m is 0.5% of M_{ship} yields excellent motion reduction. However, a mass of larger than 2% seems unnecessarily large for shipboard control systems due to the slope of the curve presented in Figure 5-12. Space and weight are of great importance in the anti-roll tank system. The added benefit from a mass larger than 0.5% of M_{ship} for the active system and 2% of M_{ship} for the passive system is negligible.

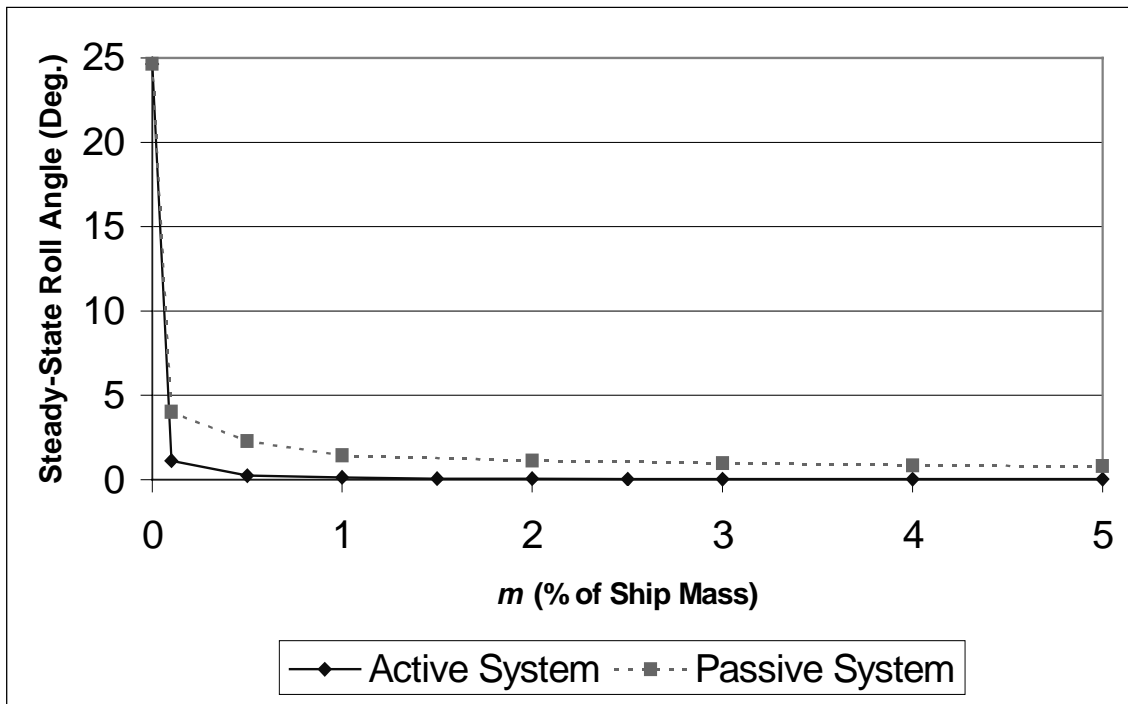


Figure 5-12. Effect of Mass (m) on Steady-State Roll Amplitude, $z_m = 0.0$

The next parameter investigated is the vertical location of the mass, z_m . In this study, z_m is varied for values that correspond to locations from approximately the keel ($z_m = -0.06$) to the deck ($z_m = 0.05$) on the Series 60, $CB = 0.7$ ship. The effect of the vertical location on the steady-state roll angle is investigated for both the active and passive systems. The results from the variation of z_m are presented in Figure 5-13.

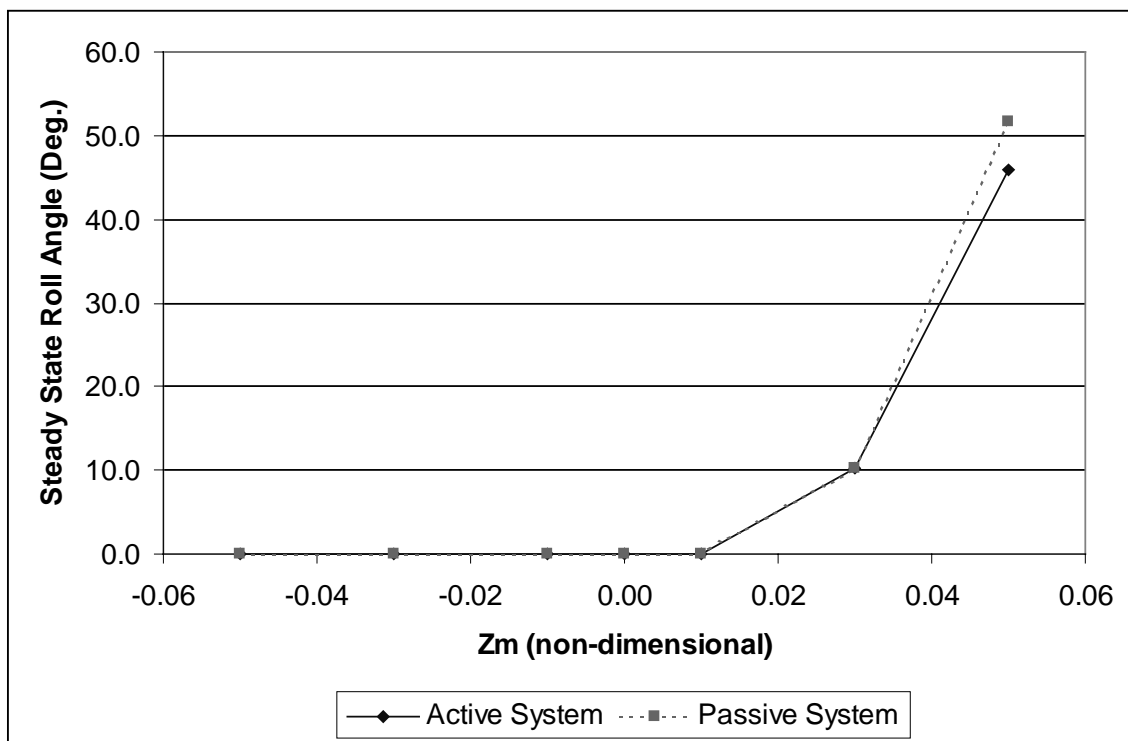


Figure 5-13. Effect of Z_m on Steady-State Roll Amplitude, $m = 2\% M_{ship}$

In Figure 5-13, the steady-state roll angle is shown as a function of the vertical location of m . The location of m has a negligible effect on the steady-state roll amplitude until the value of z_m goes positive. As described in section 3.3.2 and seen in Figure 3-3, z_m is measured positive upward from point O (see Figure 3-3), which corresponds to the center of gravity of the ship in the MOTSIM formulation. As the mass is positioned above the Cg, the influence of the mass tends to destabilize the system. For this reason, the centerline of the anti-roll tank system should be positioned below the Cg of the ship.

The effect the maximum distance in the transverse direction that m can move, d_{max} , is also investigated. The value of d_{max} is varied from an initial value of 10% to 95% of the half-beam on the Series 60, CB = 0.7 ship. In Figure 5-14, the results of this study are shown.

In Figure 5-14, the steady-state roll amplitude is presented as a function of d_{max} in the prescribed range. The effect of varying d_{max} is almost negligible for the active system. The passive system, however, is slightly more responsive than the variation of d_{max} . This figure also shows that it may not be necessary to have the mass move the entire width of the ship. In the physical anti-roll tank system, this means that the tanks in the system may not need to be placed very far apart, which allows for flexibility in the arrangement of the tanks and could make it easier to actively pump.

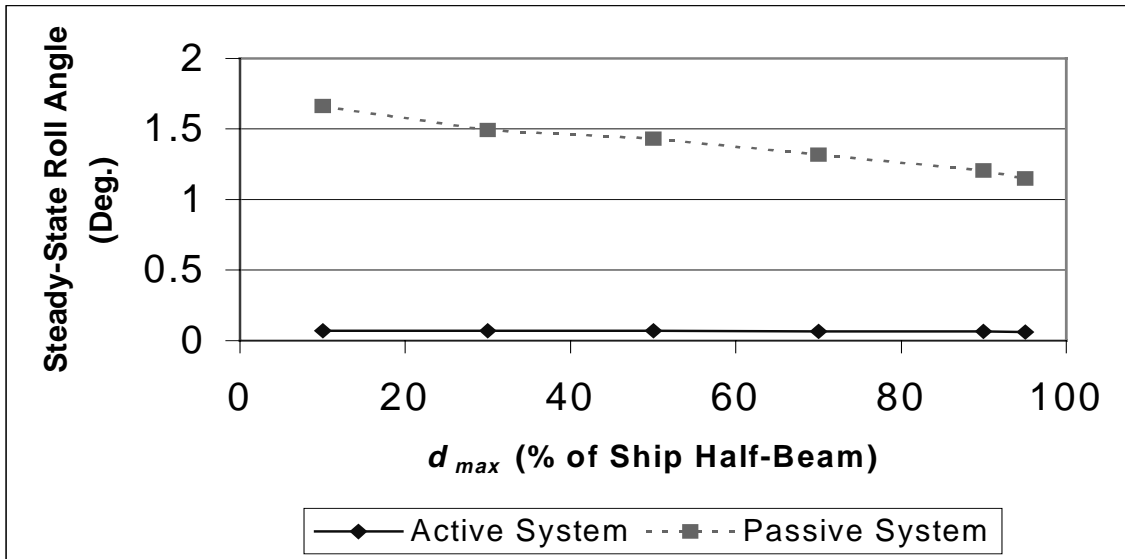


Figure 5-14. Effect of d_{max} on Steady-State Roll Amplitude, $m = 2\% M_{ship}$, $z_m = 0.0$

5.3 Installation of a Two-Degree-of-Freedom Active System in LAMP

The two-degree-of-freedom, active-tank approximation discussed in section 3.2 is used to validate the feasibility of using the LAMP program to study the effects of an anti-roll tank system as the ship is free to move in all six degrees of freedom. The ship is given an initial displacement or a beam sea case as a means of identifying the amount of control authority produced by the moving mass. These cases also proved to be an effective means of initially testing the subroutine structure used to insert the forces and moments produced by the motion of the mass into the LAMP code. The following case descriptions are results generated from LAMP simulations. Please note that the ship moves in all six degrees of freedom, and the roll angle described in all of the LAMP calculations refers to the Euler angle about the x-axis of the ship-fixed system.

5.3.1 Ship Response, Without Roll Control

The history of the motion for the Series 60, $CB = 0.7$ ship with no control for the initial displacement and wave excited cases are presented in this section for easy reference. In Figure 5-15, the results are shown for a ship given an initial displacement in roll of approximately 16 degrees and allowed to freely oscillate. For the time record shown in this plot, the roll motion decays at a very slow rate.

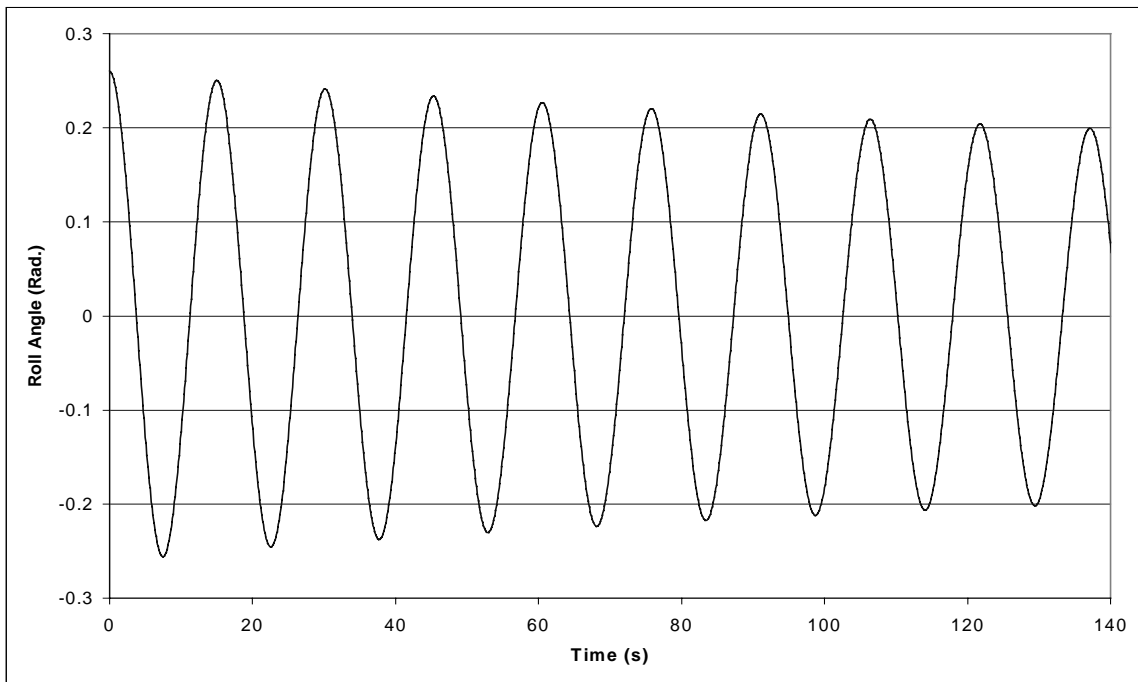


Figure 5-15. History from LAMP Calculation for a Ship Following an Initial Displacement in Roll without Control

In Figure 5-16, the motion history is shown for the beam sea case where a steady-state roll amplitude of approximately 0.33 radians (19 degrees) is obtained. The oncoming waves for this case have a non-dimensional amplitude of 0.03, a non-dimensional frequency of 1.468, and come from the beam side. All of the beam-sea cases tested in LAMP use these wave settings.

It may also be noticed in Figure 5-16 that there is a slight bias of the roll amplitude. The roll bias is a result of the course-keeping autopilot in LAMP causing the rudder to oscillate about a non-zero deflection angle. The non-zero rudder deflection imparts a slight roll moment that in turn produces a roll angle as the autopilot attempts to maintain the ship's heading in the beam sea condition. In Figure 5-17, the commanded rudder angle and the actual rudder angle are plotted as functions of time. The roll bias is noticed in all of the LAMP beam sea cases shown in this paper.

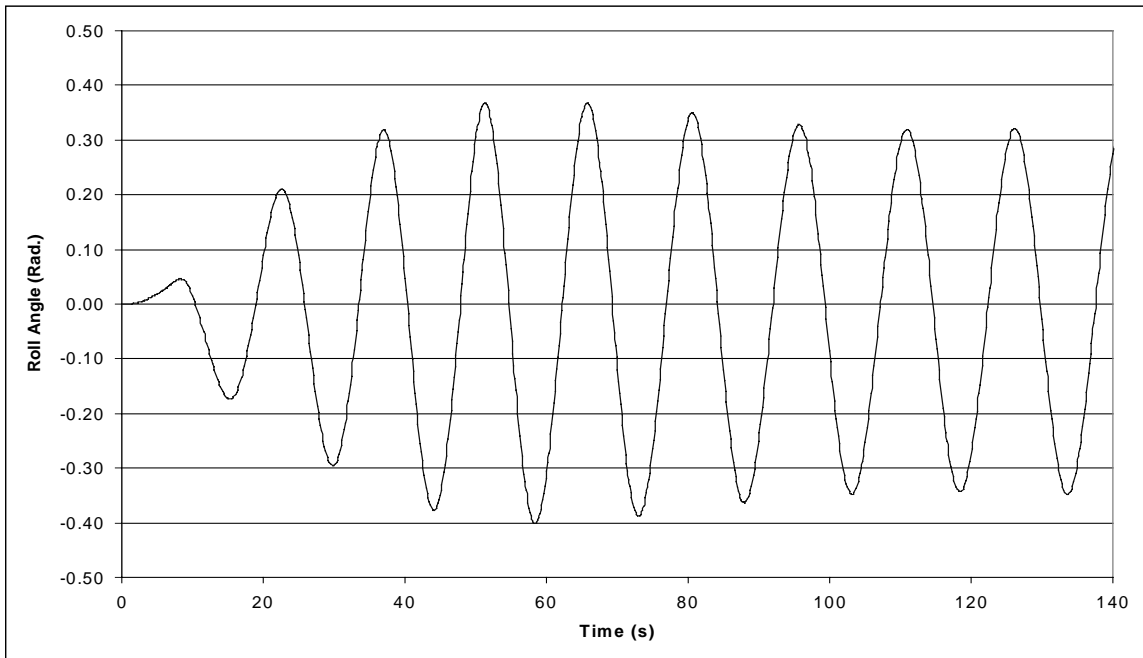


Figure 5-16. History of the Wave-Excited Motion from LAMP Calculation for a Ship without Roll Control

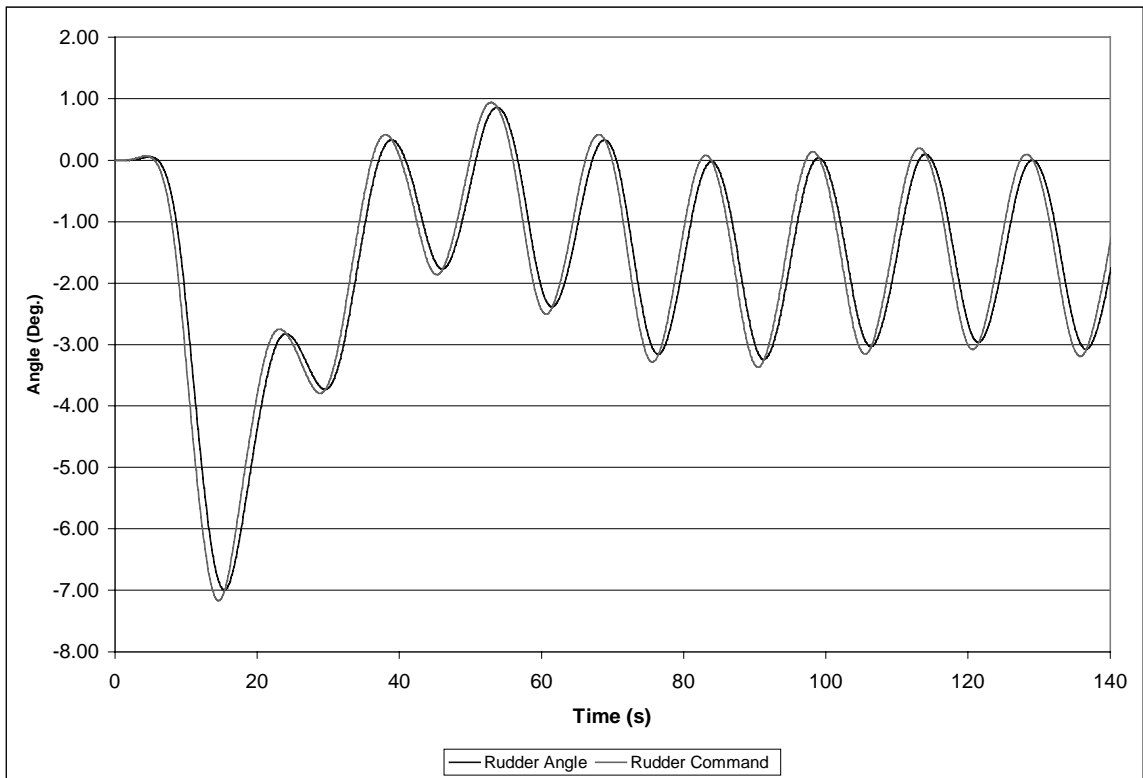


Figure 5-17. History of Course-Keeping Rudder Motion for a Wave-Excited Ship without Roll Control

5.3.2 Initial Displacement Case

Three cases are run for a Series 60, $CB = 0.7$ ship in calm seas where the ship is given an initial displacement in roll of ten degrees. The mass approximating the fluid in the tanks is 0, 2, and 0.8 percent of the ship mass (M_{SHIP}). The ship is then allowed to oscillate in all six degrees of freedom, and the time history of the roll motion is presented in Figure 5-18. The other 5 degrees of freedom are not presented here since there is little variation in the time history for the controlled and uncontrolled cases.

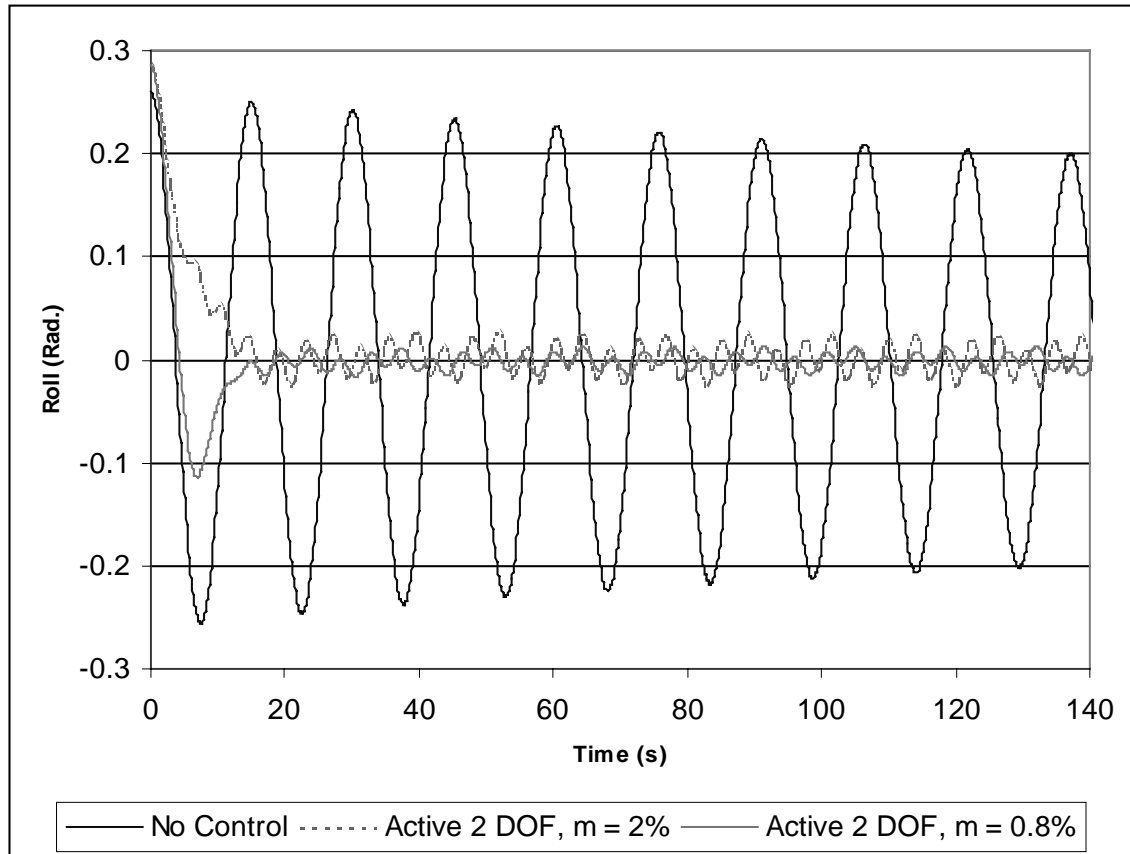


Figure 5-18. Roll Histories for 3 Cases Following an Initial Displacement with No Wave Excitation for the 2 Degree-of-Freedom Active-Tank Approximation

In Figure 5-18, the roll motion for the zero-percent mass case is shown to have a very slow decay indicating that the LAMP program has very little damping in the roll degree of freedom. LAMP is a potential-flow program in which the effects of viscosity are neglected. However, the settings used for this and the remaining LAMP runs add the influences of skin friction as well as the damping force from bilge keels (See section 2.3.) The ship motion in roll is still weakly damped even with the addition of these additional damping forces in LAMP.

The history of the motion when m is increased to 2.0 or 0.8 percent of M_{ship} shows a significant reduction in the amplitude of the roll motion. However, there is a high frequency oscillation in the motion, which is due in part to the lack of sophistication in the active control law and the parameters used in the servomechanism. The parameters for the servomechanism and the active controller are identical to the ones in the MOTSIM

formulation presented in section 5.2.2, but the MOTSIM results for the initial displacement case (Figure 5-5) show no high frequency oscillation. This indicates that the number of degrees of freedom has some influence on the behavior of the active control law. In essence, the active controller is over-compensating for the ship motion. The fact that the mass influences only the roll and sway degrees of freedom for this preliminary approach is somewhat physically unreasonable. However, this preliminary formulation shows the validity of the implementation of the anti-roll tank algorithm in the LAMP code as the ship is free to move in all six degrees of freedom. In Figure 5-18, it is shown that significant roll reduction is predicted by the point-mass approximation. The 0.8 and 2 percent mass cases also give us a “ballpark” range for the amount of the mass necessary to yield significant control authority.

5.3.3 Forced Motion Case (Beam Sea)

The Series 60, CB = 0.7 ship is run in a beam sea where the frequency of the single sinusoidal wave is equal to the natural frequency of the ship in roll, the worst case. The amplitude of the wave is sufficient to cause significant roll amplitude. Three time histories are presented for all six degrees of freedom in Figure 5-19, where the moving mass is 0, 0.8, and 2 percent of the ship’s displaced mass (M_{SHIP}).

For the case with no control (zero percent mass), the average amplitude in roll is approximately 0.33 radians. The cases of 2 and 0.8 percent mass show roll reductions of approximately 85 and 84 percent, respectively, for the selected PID controller gains. Identical gains were used for each of these two cases. The G_3 value was selected from a trial-and-error method for this initial investigation, but a more thorough investigation of gain settings is carried out in section 5.2.2.1. The sway, pitch, and yaw motions shown in Figure 5-19 indicate that m has some effect on these degrees of freedom. The most interesting effect is seen in pitch, where a significant pitch reduction is noticed. As with the initial displacement case discussed in the previous section, the methodology for implementing the anti-roll tank system approximation in the LAMP code appears to be valid.

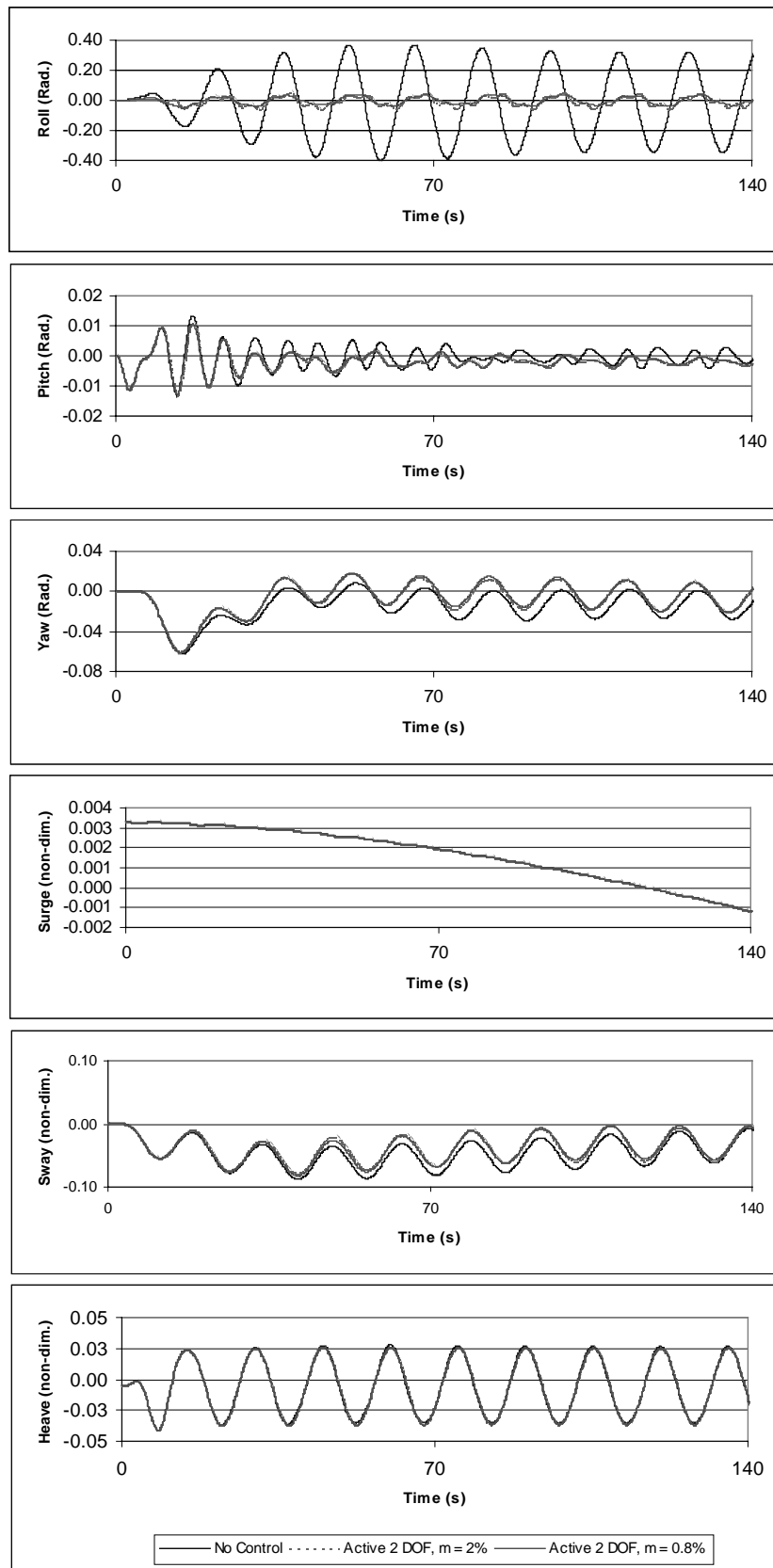


Figure 5-19. Wave-Excited Roll History from LAMP Calculation for the 2 Degree-of-Freedom Active-Tank Approximation

5.4 Installation of the Six-Degree-of-Freedom Systems in LAMP

5.4.1 Active System Implementation

The six-degree-of-freedom active system installed in the LAMP program is described in detail in section 3.3. The Series 60, CB = 0.7 hull form is used to generate the following results. The controller gain is exactly the same as the one used for the MOTSIM active system implementation discussed in section 5.2.2.1, and the non-dimensional value for the vertical height of the mass system is $z_m = -0.04$ (See Figure 3-3).

5.4.1.1 Initial Displacement Case

The initial displacement case roll motion shown in Figure 5-20 indicates that the active system, when formulated in six degrees of freedom, has the similar motion reduction characteristics as the two-degree-of-freedom case presented in section 5.3.2. The LAMP calculation is performed in all six degrees of freedom, and roll is considered the rotation about the x-axis of the ship-fixed coordinate system. The difference between the LAMP calculations with and without the controller is only significant in the motion; therefore only the roll motion is presented.

The active control system adds a great deal of additional damping to the system, however the roll angle returns to and oscillates about zero at a high frequency (see section 5.3.2 for discussion on this topic). The active system works reasonably well in LAMP for the case of initial displacement, yet the motion is not as smooth and regular when compared to the results shown in Figure 5-5 for the MOTSIM calculation. Future work includes a more detailed investigation into the servomechanism model and the control algorithm used in this case.

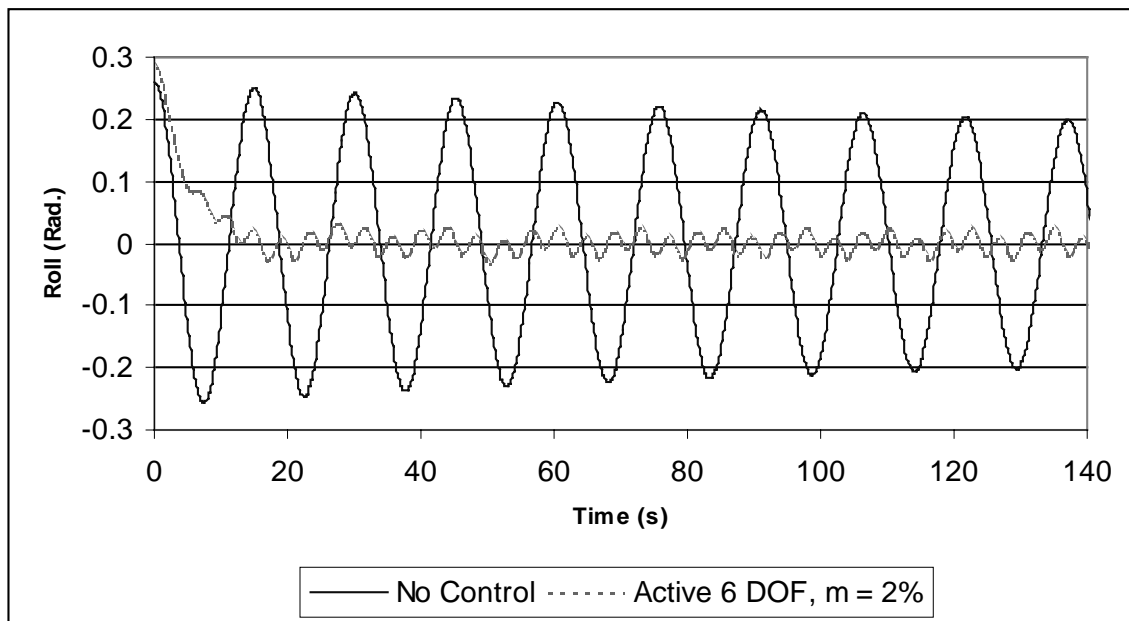


Figure 5-20. Roll Motion History from LAMP Calculation for a Ship with Active Anti-Roll Tanks Following Release from an Initial Displacement in Calm Water

5.4.1.2 *Forced Motion (Beam Sea) Case*

In Figure 5-21, the results for the beam sea case in LAMP are shown for all six degrees of freedom. The active control system reduced the steady-state roll amplitude from the 0.33 radians (19 degrees) to 0.05 radians (2.9 degrees) for an 85% reduction.

The motion seen in Figure 5-21 is not as smooth and regular as the forced motion case from the MOTSIM results shown in Figure 5-7, yet a significant reduction in roll amplitude is still attained (85% for LAMP versus 99% for MOTSIM). The effect from m on the ship motion, shown Figure 5-21, is most noticeable in the sway, roll, pitch and yaw degrees of freedom. However, m has little effect on the surge and heave motions.

The irregular roll motions from the LAMP results may be attributed to the tuning of the active controller servomechanism. The natural frequency of the active system is not the same as the natural frequency of the ship roll motion, which explains the additional frequency content in the motion. The controller natural frequency is set to a value corresponding to 10 Hz and adjusting the controller frequency may smooth out the irregular nature of the roll motion. Adjusting the damping in the servomechanism may also help smooth the response. The goal of this work was to show the system's ability to reduce the magnitude of the roll motion, but future work may include a study into the servo-system model.

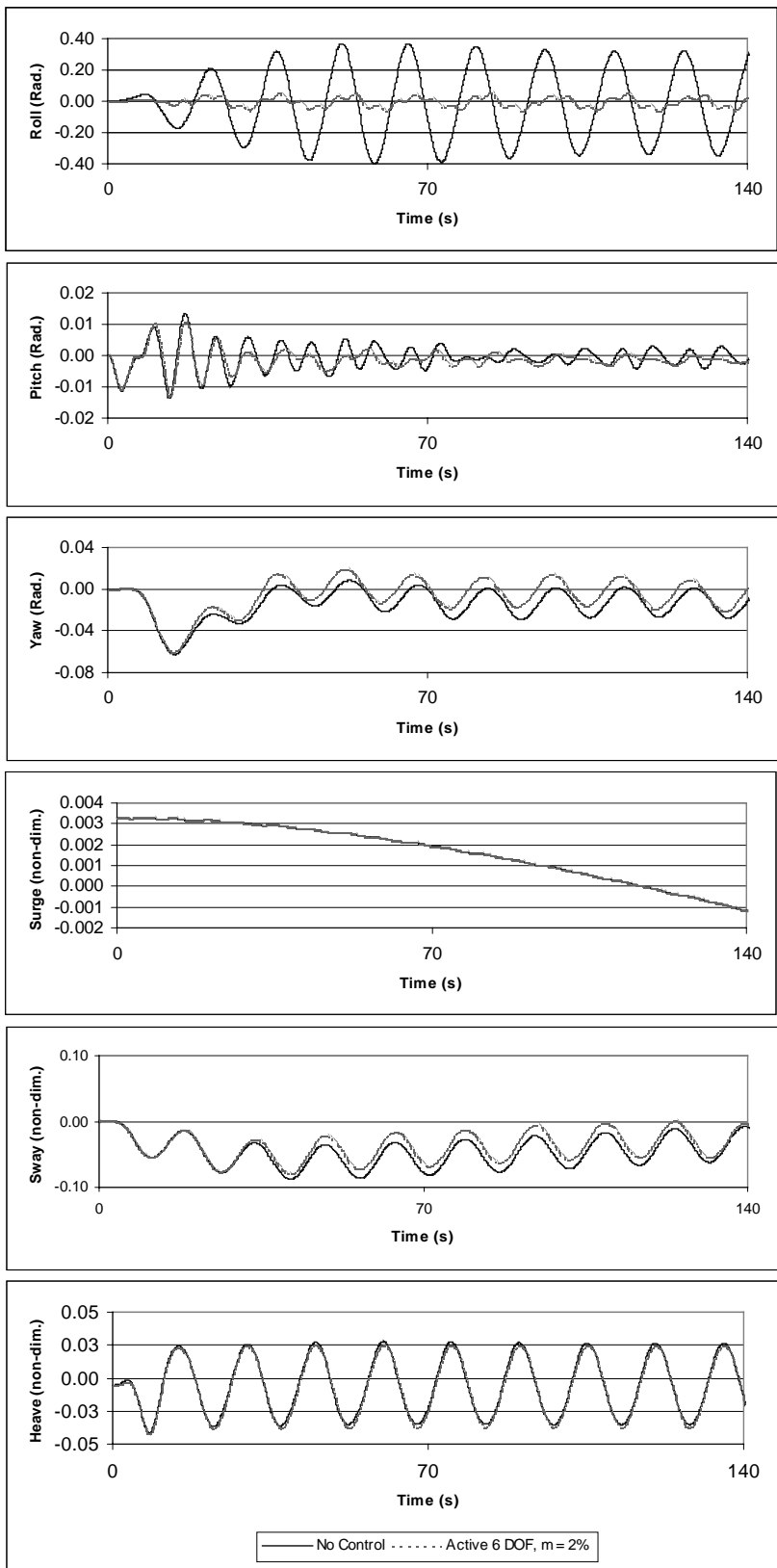


Figure 5-21. History of the Wave-Excited Motion from LAMP Calculation for a Ship with Active Anti-Roll Tanks

5.4.2 *Passive System Implementation*

The passive system discussed in this section is described in detail in section 3.4 and results from the MOTSIM program for this formulation are presented in section 5.2.3. The results shown here are generated using the Series 60, $CB = 0.7$ hull form as seen in section 5.1. The ω_m and μ_m values from the mass system equation of motion [3.15] are set to nearly the ship natural frequency ω_{ship} and 10% ω_{ship} , respectively, for both the initial displacement case and the beam sea case. The non-dimensional value for the vertical height of the mass system is set to $z_m = -0.04$ for both cases as well.

5.4.2.1 *Initial Displacement Case*

For the first test of the passive system in LAMP, the system was given an initial displacement equivalent to 16 degrees of ship roll angle and allowed to oscillate. The passive system, as described in section 4.2.2, acts as a vibration absorber that reduces the amplitude of the roll motion. The results of the passive system tested in the MOTSIM program and presented in section 5.2.3.1 showed good motion damping characteristics, but the motion settled to a non-zero roll amplitude as seen in Figure 5-9.

The LAMP calculation is performed in all six degrees of freedom. The variation between the LAMP calculations for the case with and without the controller is only significant in the roll degree of freedom; therefore only the roll motion is presented in Figure 5-22. In Figure 5-22, the roll motion settles to a zero amplitude with a regular oscillatory decay. The results suggest that the passive system in LAMP does not yield the same control authority seen in the active system (Figure 5-20). However in LAMP, the passive system does yield a more regular ship motion than the single degree-of-freedom formulation calculated in MOTSIM.

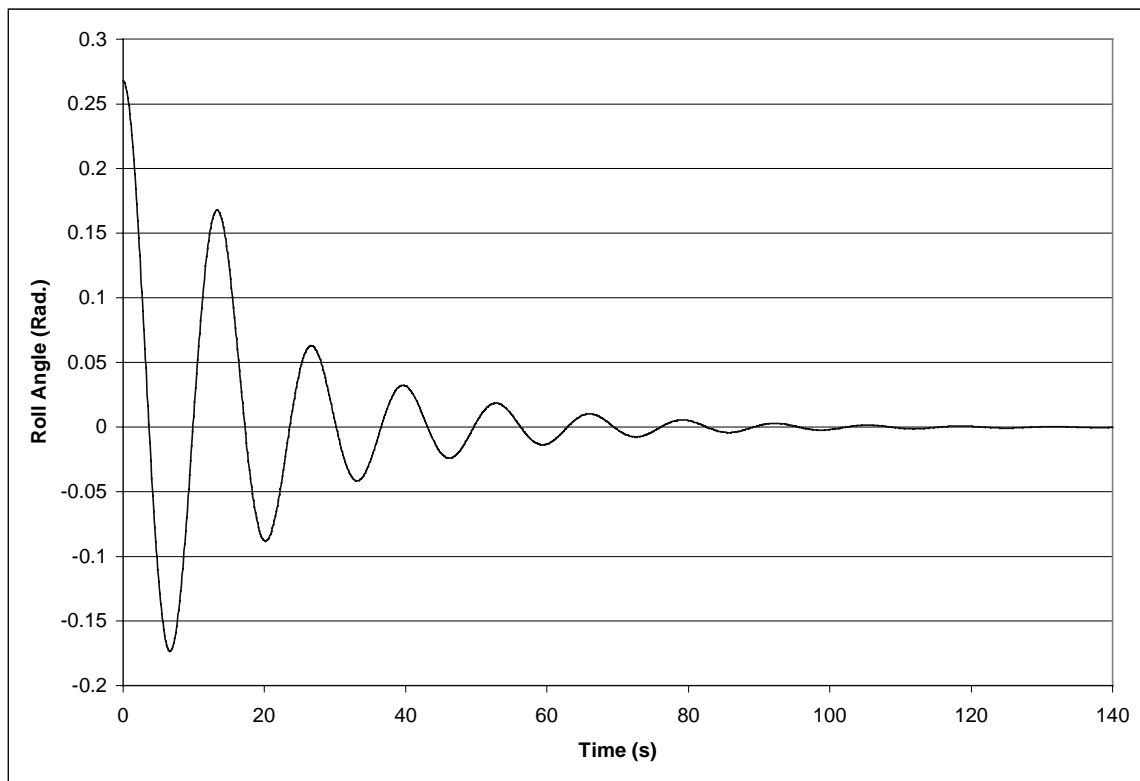


Figure 5-22. Roll Motion History from LAMP Calculation of a Ship with Passive Anti-Roll Tanks Following Release from an Initial Displacement in Calm Water

5.4.2.2 Forced Motion (Beam Sea) Case

The wave-induced motion presented in this section has the same parameters used in section 5.4.1.2 for the active controller. The performance of the passive control system is evaluated in presence of a beam sea wave as described in section 5.3.1. The steady-state roll motion with no controller present is presented in Figure 5-16, where a steady-state amplitude of approximately 0.33 radians (19 degrees) is obtained. The MOTSIM calculations for this case are presented in section 5.2.3.2.

In Figure 5-23, the calculated result from the passive control system implementation in LAMP is shown for all six degrees of freedom. In this case, an average steady-state roll amplitude of 0.16 radians (9.2 degrees) is obtained. The roll motion bias discussed in section 5.3.1 is also noticed in this calculation. The roll reduction obtained in the LAMP calculation (51% reduction) is significantly less than the calculated result in MOTSIM (95% reduction) shown in Figure 5-10. The reduced effectiveness in the LAMP calculations for the wave induced motion case shows that the passive system is sensitive to the number of degrees-of-freedom considered in the formulation, six for LAMP and one for MOTSIM.

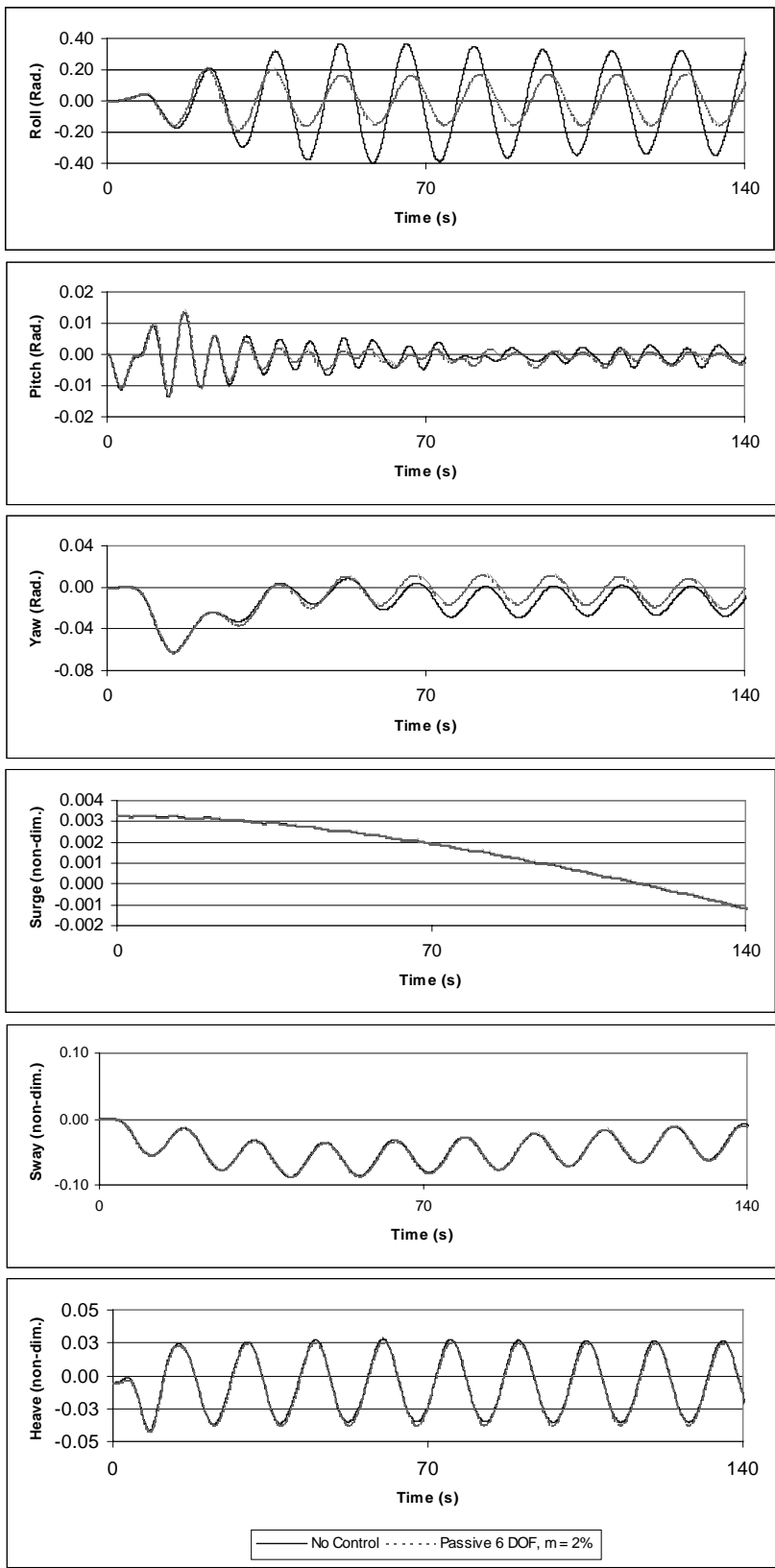


Figure 5-23. History of the Wave-Excited Motion from LAMP Calculation for a Ship with Passive Anti-Roll Tanks

5.4.3 Six-Degree-of-Freedom vs. Two-Degree-of-Freedom LAMP Models

Many authors including Webster (1967), Webster, Dalzell, & Barr (1988), and Chen, Shaw, Khalil, & Troesch (1996) use a reduced-degree-of-freedom model for the dynamics of anti-roll tank systems. As a comparison, this section presents the six-degree-of-freedom and the two-degree-of-freedom tank approximations in six-degree-of-freedom LAMP calculations. Results for the wave-excited active and passive system cases are presented. In Figure 5-24, the roll motion history for the active system formulations are shown for both the two-degree-of-freedom (see section 5.3.3) and the six-degree-of-freedom models (see section 5.4.1.2). The magnitude of the roll angle is comparable for both cases, but there is some variation in the actual time history.

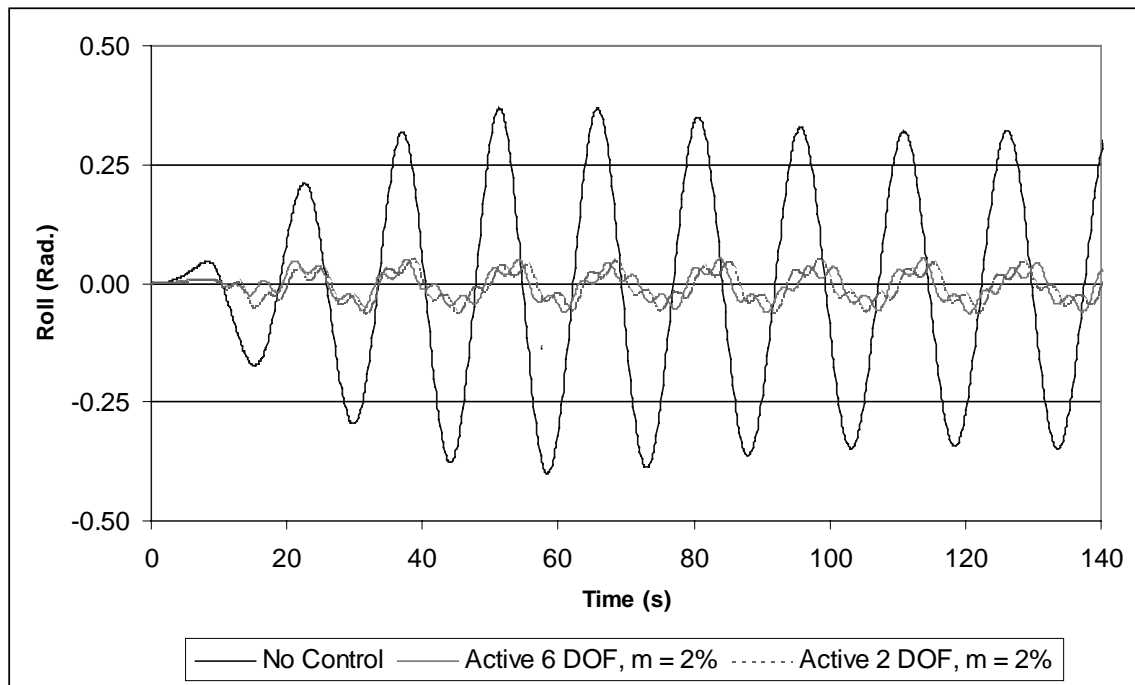


Figure 5-24. History of the Wave-Excited Roll Motions from LAMP Calculations for a Ship with Six and Two Degree-of-Freedom Active Tank Formulations

In Figure 5-25, the LAMP calculations of the roll motion for the passive system formulations are shown for both the two-degree-of-freedom and the six-degree-of-freedom models (see section 5.4.1.2). The two-degree-of-freedom passive system uses the same force in sway and moment roll as the active two-degree-of-freedom approximation equations [3.3] and [3.4], respectively. The position of the mass is found by the passive system equation [3.15].

The LAMP passive system calculations for the two-degree-of-freedom and six-degree-of-freedom approximations yield similar steady-state roll amplitudes. However, the two-degree-of-freedom approximation has a slight phase lag to the six-degree-of-freedom approximation.

The comparison of the two-degree-of-freedom and six-degree-of-freedom models for both the active and passive systems suggest that a reduced-degree-of-freedom model may work well for motion magnitude, but may not give an accurate time history of the ship motion. For cases where a more accurate time history of the ship is important, the six-

degree-of-freedom tank dynamics should be included to provide the best possible prediction of the ship motion.

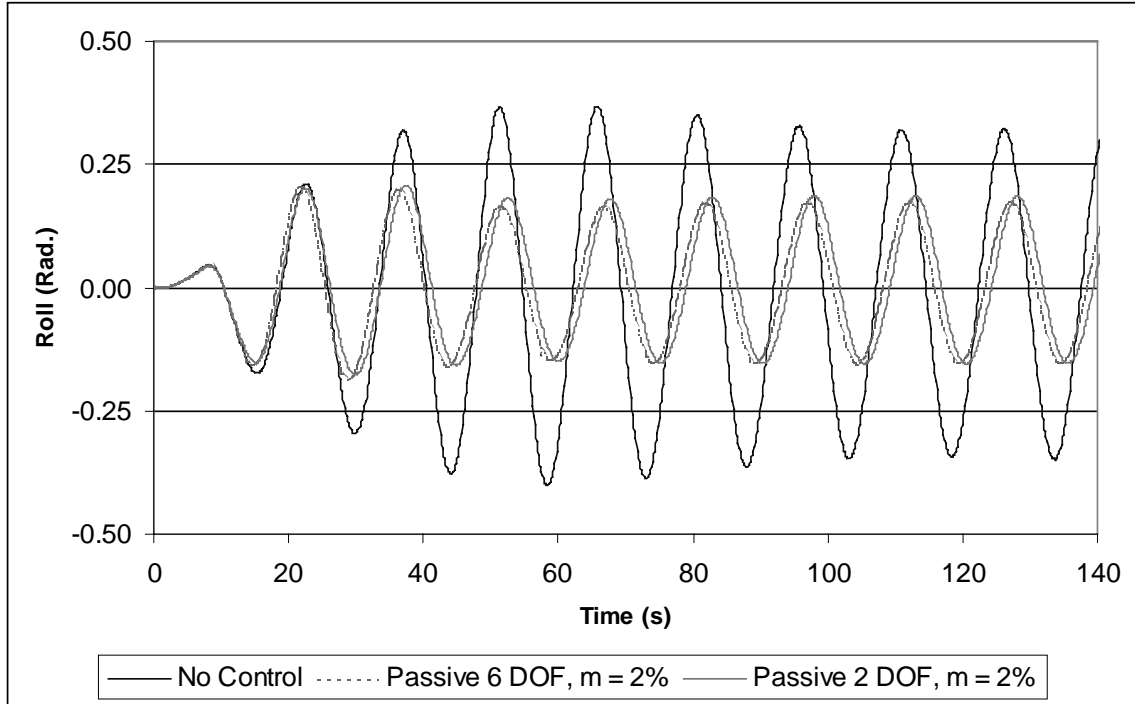


Figure 5-25. History of the Wave Excited Roll Motions from LAMP Calculations for a Ship with Six and Two Degree-of-Freedom Passive Tank Formulations

***Chapter 6* Conclusions and Recommendations for Future Work**

6.1 MOTSIM Anti-Roll Tank System Evaluation

A single degree-of freedom motion simulator, called MOTSIM, was formulated as a test platform to simulate the roll motion of a ship fitted with active and passive anti-roll-tank systems. The formulation of the MOTSIM system model was discussed in Chapter 4. Approximations were made to the equation of motion in the roll degree-of-freedom, and the anti-roll tank system was approximated by a moving point mass. MOTSIM was tuned so that the output closely matched the roll motion history of the Series 60, CB = 0.7 hull form predicted in LAMP calculations. The result was a program that runs many times faster than the LAMP program and which allowed numerous long-time runs to be made.

6.1.1 Active Anti-Roll-Tank System in MOTSIM

A root-locus technique was used to find the gains for the PID controller used in the active-system formulation. The active anti-roll system was used to evaluate two primary cases. In the first case presented in section 5.2.2.2, the ship was given an initial displacement of 16 degrees of roll and allowed to oscillate. Figure 5-5 showed a comparison of calm water roll history following an initial-displacement with no control, and a case where the moving mass (m) was equal to 2% of the total ship mass (M_{ship}). The MOTSIM calculation showed that the active controller reduced the roll motion to zero degrees with no oscillation. The results in Figure 5-5 showed that the roll motion may be damped by using an active system where the commanded position of the mass is proportional only to the roll velocity of the system as described in section 3.2.2.2. The results also showed that sufficient control authority was generated when m was 2% of M_{ship} .

In the second case investigated, the ship was subjected to a sinusoidal forcing function, which approximated a wave excitation. The encounter frequency of the forcing function was also nearly equal to the ship's natural frequency in roll, a condition that produces the largest steady-state amplitudes. Figure 5-6 showed that when no control is applied to the system, a steady-state amplitude of 0.43 radians (25 degrees) was obtained. With the controller activated, the steady-state amplitude of the system was reduced to 1.1×10^{-3} radians (0.06 degrees) as shown in Figure 5-7. The 99% roll amplitude reduction seen in Figure 5-7 suggests that the active system with m equivalent to 2% of M_{ship} yields very favorable, although somewhat optimistic, motion characteristics. The results must be considered optimistic since the roll-damping model used in the LAMP code may under-predict the actual roll damping seen by the ship.

6.1.2 Passive Anti-Roll Tank Systems in MOTSIM

MOTSIM was also used to simulate a passive system for two test cases. For the first case, the ship was given an initial displacement equivalent to 16 degrees of roll and allowed to oscillate in calm water. The passive system acted as a vibration absorber. In Figure 5-9, a comparison was shown of the roll motion history for a case with no control and a case where the moving mass (m) is equal to 2% of the total ship mass (M_{ship}). The passive system does not seem to work very well for the initial displacement case. The motion does

decay, but the resulting equilibrium position was non-zero. The passive system lost its effectiveness as the oscillations of the roll motion decay.

For the second case, a sinusoidal forcing function was acted on the ship. The encounter frequency of the forcing function was nearly equal to the natural frequency in roll, a condition that produces the largest steady-state amplitude. The forcing function caused the system to reach a steady-state roll amplitude of 0.43 radians (25 degrees) with no controller present. Figure 5-10 showed the effectiveness of the passive system in the forced motion case with $m = 2\% M_{ship}$ where the roll motion was reduced to approximately 0.02 radians (1.15 degrees), a 95% reduction. The passive system was very effective in absorbing the energy from the forcing function, and therefore the ship roll motion was reduced.

6.1.3 MOTSIM Coefficient Influence Study

A study was performed to find the influence on the motion of several of the terms used in the MOTSIM formulation. The active and passive systems were used to perform an investigation that consisted of the variation of system parameters such as m , z_m , and d_{max} .

Figure 5-12 shows the results on the steady-state roll amplitude from varying the value of m . It was concluded that even for the case where m was 0.5% of M_{ship} , excellent motion reduction was obtained, and a mass of larger than 2% seems unnecessarily large for shipboard control systems. Space and weight are of great importance in the consideration of an appropriate anti-roll tank system, and the added benefit from a mass larger than 2% of the ship mass was negligible.

The next parameter investigated was the vertical location of the mass; z_m was varied from approximately the keel to the deck on the Series 60, CB = 0.7 ship. The effect of the vertical location on the steady-state roll angle was investigated for both the active and passive systems. The results are presented in Figure 5-13. The vertical location of m has only a negligible effect on the steady-state roll amplitude until the value of z_m goes positive. When the mass was positioned above the Cg, its influence tended to destabilize the system. For this reason, the centerline of the anti-roll tank system should be positioned below the Cg of the ship or maybe the control gains needed to be changed.

The effect of the physical constraint on the maximum distance in the transverse direction that m can move, d_{max} , was also investigated. The value of d_{max} was varied from an initial value of 10% to 95% of the half-beam on the Series 60, CB = 0.7 ship. Figure 5-14 showed the result of this study and suggested that the mass need not move the entire width of the ship. In the physical anti-roll tank system this means that the tanks in the system may not need to be placed very far apart, which allows for flexibility in the arrangements.

6.1.4 Recommendations for Future Development

Future developments in the MOTSIM program may be made in several areas. First, as the model of roll damping in the LAMP program improves, the MOTSIM damping model may be expanded to include additional linear and nonlinear terms proportional to the roll velocity, the roll acceleration, and the square of the velocity. Improving the roll-damping model is essential to improving the accuracy of the simulations.

The MOTSIM formulation may also be expanded to a nonlinear six-degree-of-freedom model in future versions. This is a very extensive task due to the coupling of the

various degrees of freedom. Determining the coefficients for the coupled equations will not be as straightforward as tuning the roll-only equation presented in this paper, yet once these coefficients are determined for a given hull form the computational power needed to have a nonlinear real-time ship-motion simulator currently exists. Such a simulator could vastly improve the control of ships and expand their operational regime.

6.2 LAMP Anti-Roll Tank System Evaluation

The LAMP program was modified and used as a simulator to evaluate the effectiveness of anti-roll tank systems in the time-domain. Subroutines were added to LAMP, which calculate the effects of both active and passive anti-roll systems on a ship. The formulation for the implementation of these systems was discussed in detail in Chapter 3.

6.2.1 Active Anti-Roll Tank Systems in LAMP

The active-system implementation in LAMP was initially formulated by using a two-degree-of-freedom dynamic approximation, which is discussed in section 3.2. This formulation is used to verify the subroutine logic required in LAMP program structure. Figure 5-18 presented the results from three cases of varying mass for the Series 60, CB = 0.7 ship in calm seas. For these cases, the ship is given an initial displacement in roll of ten degrees and allowed to oscillate. The history of the motion when m is increased to 2 or 0.8 percent shows that there is a significant reduction in the amplitude of the roll motion. However, there is a high frequency oscillation in the motion, which is due in part to the lack of sophistication in the active control law and the parameters used in the servomechanism. The parameters for the servomechanism and the active controller were identical to the ones in the MOTSIM formulation presented in section 5.2.2, but the MOTSIM result from the initial displacement case (Figure 5-5) shows no high frequency oscillation. This suggests that the number of degrees of freedom used has some influence on the behavior of the active control law. This preliminary simulation showed the validity of the anti-roll algorithm in the LAMP code as the ship is free to move in all six degrees of freedom. In Figure 5-18, it was shown that significant roll reduction might be obtained by using the point-mass approximation.

The two-degree-of-freedom implementation was also verified using a single sinusoidal wave with a frequency nearly equal to the roll natural frequency of the ship. The amplitude of the wave is sufficient to cause significant roll. Three time histories were presented for the active control formulation in Figure 5-19, where favorable roll motion reduction was also obtained. The relative success of these initial two-degree-of-freedom studies verified that the subroutine logic in LAMP is working correctly.

The six-degree-of-freedom formulation discussed in section 3.3 was used to simulate two cases. In the first case, the ship was given an initial displacement in roll and was allowed to oscillate in calm water. In the second case, the motion was excited by a beam-sea wave and the ship was free to move in all six degrees of freedom. The active system utilized the same controller gains presented in section 5.2.2.1 where a root locus technique was utilized to find stable gains. The results for the first case presented in Figure 5-20, show that the active control system added a great deal of additional damping to the system and the roll angle returned to and oscillated about zero. The high frequency oscillation in the LAMP calculation shows the need to investigate more sophisticated control algorithms.

In Figure 5-21, the results for the wave-excited motion predicted by LAMP were shown. The active-control system reduced the steady-state roll amplitude from the 0.33 radians (19 degrees) seen in Figure 5-16 to 0.05 radians (2.9 degrees), an 85% reduction. However, the motion was not very smooth and regular compared to the forced motion predicted by MOTSIM and shown in Figure 5-7, yet a significant reduction in the predicted roll amplitude was still attained. The irregular nature of the ship roll motions from the LAMP calculation may be attributed to the tuning of the active controller servomechanism. The natural frequency of the active system is also not similar to the natural frequency of the ship roll motion, which explains the additional frequency content seen in the motion history.

6.2.2 *Passive Anti-Roll Tank Systems in LAMP*

The passive system was implemented in LAMP for the six-degree-of-freedom dynamics in section 3.4 and results were presented in section 5.2.3. For the first case tested of the passive system in LAMP, the system was given an initial displacement equivalent to 16 degrees of roll and allowed to oscillate in calm water. The passive system acted as a vibration absorber and reduced the amplitude of the roll motion. The LAMP calculation for the initial displacement case presented in Figure 5-22, showed that the roll motion does settle to zero amplitude with a regular oscillatory decay. The oscillation of the ship suggested that the passive system in LAMP does not yield the same control authority as the active system for the initial displacement case shown in Figure 5-20. However, the passive system does yield a more regular ship motion than the single degree-of-freedom formulation calculated in MOTSIM and presented in Figure 5-9.

The wave-induced motion was simulated in the presence of a beam sea as described in section 5.3.1. In Figure 5-23, the calculated results for the passive control system in LAMP were shown for all six degrees of freedom. In this case, the average steady-state roll amplitude was reduced from 19 degrees (no control) to 9.2 degrees. There was also a noticeable bias in the roll motion in this calculation, which was discussed in section 5.3.1. The roll reduction obtained in the LAMP calculation (51% reduction) is significantly less than the calculated result in MOTSIM (95% reduction) shown in Figure 5-10. The reduced effectiveness in the LAMP calculations for the wave induced motion showed that the passive system was sensitive to the number of degrees-of-freedom considered in the formulation, six for LAMP and one for MOTSIM. However, the 51% roll reduction predicted by the LAMP calculation was consistent with the published results from Sellars & Martin (1992), where reductions of 40-60% were attained with a tank sized to be 1-2% of the ship displacement.

6.2.3 *Comparison of System Models*

Results for the wave-excited cases for both the active and passive systems were presented in section 5.4.3. In Figure 5-24, the roll motion history for the active system were shown for both the two-degree-of-freedom (see section 5.3.3) and the six-degree-of-freedom models (see section 5.4.1.2). The magnitude of the roll angle was comparable for both cases, but there was some variation in the actual time history.

In Figure 5-25, the LAMP calculations of the roll motion for the passive system formulations were shown for both the two-degree-of-freedom and the six-degree-of-freedom models (see section 5.4.1.2). The passive-system calculations for the two-degree-of-freedom and six-degree-of-freedom approximations yield similar steady-state roll

amplitudes. However, the two-degree-of-freedom approximation has a slight phase lag to the six-degree-of-freedom approximation. The comparison of these two models for both the active and passive systems suggests that a reduced-degree-of-freedom model may predict the motion amplitude well, but may not give an accurate time history. For cases where a more accurate time history of the ship is important, the six-degree-of-freedom tank dynamics should be included to provide the best possible prediction. In Table 6-1, a listing of the percent roll reduction is presented for all of the active and passive tank formulations presented in this paper.

**Table 6-1. Roll Reduction Percentages for Systems in Wave-Excited Conditions
where $m = 2\% M_{ship}$**

| | MOTSIM | LAMP 2 DOF | LAMP 6 DOF |
|---------------------|--------|------------|------------|
| Active Tank System | 99% | 85% | 85% |
| Passive Tank System | 95% | 51% | 51% |

6.2.4 Recommendations for Future Development

Several areas of the anti-roll tank implementation in LAMP may be candidates for future development. First, a more detailed servomechanism model for the active system formulation should be introduced into LAMP, where the dynamics of the motors are included. Also related to the servo model may be a systematic evaluation of the effects that the damping and frequency terms in the servo model have on the motion.

Future implementations should include the dynamics of the actual fluid moving in the tank system. The viscous effects of the fluid moving in the connecting pipes and the geometry of specific tank configurations should be taken into account. The LAMP input files may eventually be modified to allow a designer to locate passive or active tank systems in numerous areas of the ship and evaluate the performance of any tank configuration.

The current subroutine structure in LAMP also allows for various control methods to be used. For example, an active method for adjusting the frequency of the passive system may be evaluated which would allow the system to be tuned to a frequency near that of the oncoming waves in a given sea state. The use of a nonlinear controller, such as the one presented by Chen, Shaw, Khalil, and Troesch (1996) could also be implemented in the current structure of the LAMP subroutines. In fact, the use of any type of control algorithm may be implemented in a fairly straightforward manner.

The current damping model in the LAMP program may also be improved. Since LAMP is a potential-flow code, the viscous effects in roll, which account for most of the damping, are only empirically included. Future work may include some two dimensional viscous flow calculations from such programs as FANS (Finite Alytic Reynolds-Averaged Navier Stokes) over various portions of the hull surface. The viscous forces from these calculations could be passed to LAMP to give a more accurate representation in roll.

Finally, the use of the subroutines developed for the calculation of the active and passive anti-roll tanks is not limited to the LAMP program. As newer and more accurate time-domain codes are developed, the subroutines for the tank dynamics may be easily modified to be included in these codes.

Chapter 7 References

Baitis, A.E., and Schmidt, L.V., (1989), "Ship Roll Stabilization in the U.S. Navy", *Naval Engineers Journal*, pp. 43-53

Beck, R.F. & Liapis, S.J. (1987), "Transient motion of floating bodies at zero forward speed," *Journal of Ship Research*, Vol 31, pp. 164-176

Bell, J. and Walker, W.P, (1966) "Activated & Passive Controlled Fluid Tank System for Ship Stabilization", *The Society of Naval Architects and Marine Engineers Transactions*, Vol. 74, pp. 150-189

Carnahan, B., Luthor, H.A., and Wilkes, J.O., (1969), *Applied Numerical Methods*. John Wiley & Sons, Inc., 309-403.

Chang, M.-S., (1977) "Computations of Three-Dimensional Ship-Motions with Forward Speed", *Second International Conference on Numerical Ship Hydrodynamics*, University of California, Berkeley, September.

Chen, S.-L., Shaw, S.W., Khalil, H.K., Troesch, A.W., (1996), "Robust Stabilization of Large Amplitude Ship Rolling in Regular Beam Seas," *Nonlinear Dynamics and Controls*, DE-Vol. 91, ASME, pp. 93-98

Cummins, W.E., (1962), "The Impulsive Response Function and Ship Motions", *Schiffstechnik*, No. 9: 124-135

Den Hartog, J. P., (1985), *Mechanical Vibrations*, Dover Publications, Inc. New York

Field, S.B. & Martin, J.P., (1975), "Comparative Effects of U-Tube and Free Surface Type Passive Roll Stabilization Systems," *Spring Meeting of the Royal Institution of Naval Architects*, London, England.

Finkelstein, A., (1957), "The initial value problem for transient water waves", *Comm. Pure and Applied Mathematics*, Vol. 10.

Fossen, T.I., (1995) *Guidance and Control of Ocean Vehicles*. John Wiley & Sons, New York.

Froude, W., (1868), "Observations and suggestions on the subject of determining by experiment the resistance of ships", *The Papers of William Froude*.

Housner, Bergman, Caughey, Chassiakos, Clause, Masri, Skelton, Soony, Spencer, and Yao, "Structural Control; Past, Present, and Future", (1997), *Journal of Engineering Mechanics*, Vol 123, No. 9.

Inoue, R., Kanyama, T., & Kanaji, H., (1994), "Vibration Control of Existing Buildings Under Motion Excited by Moving Vehicles", *Proc. of First World Conference on Structural Control*, Vol 2.

King, B.W. (1987), "Time-domain analysis of wave exciting forces on ships and bodies," Report No. 306, Department of Naval Architecture and Marine Engineering, University of Michigan, Ann Arbor, Michigan.

King, B.W., Beck, R.F. & Magee, A.R., (1988), "Seakeeping Calculations with Forward Speed Using Time Domain Analysis", *Proceedings of the 17th Symposium on Naval Hydrodynamics*, The Hague, Netherlands.

Korsmeyer, F.T., (1988), "The First and Second Order Transient Free-Surface Wave Radiation Problems", Ph.D Thesis, Dept. of Ocean Engineering, MIT, Cambridge, Massachusetts.

Liapis, S.J. (1986), "Time-domain analysis of ship motions," Report No. 302, Department of Naval Architecture and Marine Engineering, University of Michigan, Ann Arbor, Michigan.

Lin, W.M., and Yue, D.K.P. (1990), "Numerical Solutions for Large-Amplitude Ship Motions in the Time-Domain," *Proceedings of the Eighteenth Symposium on Naval Hydrodynamics*, The University of Michigan, Ann Arbor, Michigan, pp. 41-65

Lin, W.-M., Zhang, S., Meinhold, M., Weems, K., "LAMP Version 283 User's Manual", SAIC Internal Report.

Minorsky, N. (1941), "Note on the Angular Motion of Ships", *Transactions of ASME*, A 69, pp. 111-120

Mitchell, J.H., (1898), "The Wave Resistance of a Ship", *Philosophy Magazine*, No. 45, pp. 106-123

Nakos, D.E. & Sclavounos, P.D. (1990), "Ship motions by a three-dimensional rankine panel method," *18th Symposium on Naval Hydrodynamics*, Ann Arbor, Michigan.

Salvesen, N., Tuck, E.O., & Faltinsen, O., (1970) "Ship Motions and Sea Loads", *The Society of Naval Architects and Marine Engineers Transactions*, Vol. 78, November. pp. 250-287

Sellars, F.H. and Martin, J.P., (1992), "Selection and Evaluation of Ship Roll Stabilization Systems," *Marine Technology*, Vol. 29, No. 2, April, pp.84-101

Shahian, Bahram and Hassul, Michael (1993), *Control System Design Using MATLAB®*. Prentice-Hall.

Stoker, J.J. (1957), "Water Waves," *Pure and Applied Mathematics*. Volume IV.

Tamura, Y., Fujii, K., Ohatsuki, T., Wakahara, T., & Koshaka, R., (1995), "Effectiveness of Tuned Liquid Dampers Under Wind Excitations", *Engineering Structures*, Vol. 17.

Vasta, J., Giddings, A.J., Taplin, A., and Stilwell, Capt. J.J. (1961), *Proceedings from the Annual Meeting of The Society of Naval Architects and Marine Engineers*, New York, NY. Pp. 411-460

Webster, W.C., (1967), "Analysis of the Control of Activated Antiroll Tanks", *Proceedings from the Annual Meeting of The Society of Naval Architects and Marine Engineers*, New York, NY. Pp.296-325

Webster, W.C., Dalzell, J.F., and Barr, R.A., (1988) "Prediction and Measurement of the Performance of Free-Flooding Ship Antirolling Tanks", *The Society of Naval Architects and Marine Engineers Transactions*, Vol. 96, pp. 333-360

Appendix A: Sample Input File for Series 60, $C_B=0.7$ in Beam Sea

```

!01 DESCR - Descriptive Title (max 80 char)
Input for free floating Series 60, CB = 0.7, Cb70 (S70) ship in wave, Fn
= 0.20
!02 FPROG - Source file for Programmers Input (blank for defaults)
cdms.prg
!03 FAPLT - Source file for Autopilot Input (blank for defaults)
olddyn.aplt
!04 FGEOM - Source file for geometry definition
s70lmp.01
!05 FOUT - Destination file for primary output
s60_70.out
!06 Output frequency for pressure, geometry, etc.
!      POUT      GOUT      SOUT      BOUT
      0 0 0      0 0 0      0 0 0      0 0 0
!07 FPOUT = File for pressure data output if POUT>0

!08 FGOUT = File for panel geometry output if GOUT>0

!09 FSOUT = File for future output if SOUT>0

!10 FBOUT = File for future output if BOUT>0

!11 IVEC - Use Non-vectorized (0) or ivectorized (1) kernel
      0
!12 LMPTYP (1/2/4)  MOTYPE (forced/impulsive/free)  MIXED (reg/mixed)
      1      2      0
!13 TINIT, NSTEP, DTH - Initial Time, Number of Steps, Time Step
      0.0      500      .04
!14 PMG(1:6) Initial location and orientation of Cg in oxyz
      .000000      .000000      -.0051843      .000000      .000000
.000000
!15 VMG(1:6) Initial Velocity and Rotation rate
      .200000      .000000      .000000      .000000      .000000      .000000
!16 AMPM(1:6) Amplitude for forced sinusoidal motion (if MOTYPE=0)
      .000000      .000000      .000000      .000000      .000000      .000000
!17 OMEGM(1:6) Frequency for forced sinusoidal motion (if MOTYPE=0)
      .000000      .000000      .000000      .000000      .000000      .000000
!18 SWITCH(1:6) Sets which modes of motion will be considered
      1      1      1      1      1      1
!19 ISEA WSPEC SIGWHT TMODAL SEAHD SPREAD NWAVES NWSC
      1      0      .000000      .000000      .000000      .000000      1      2
!19 (cont) FREQW PHASEW AMPW HEADW = component wave data
      2.000000      .000000      .040000      90.000000
!19 (cont) WSCSTP WSCFAC = wave scaling data
      0      0.0
      50      1.0
!20 GRAVIN RHOIN LENIN ANGIN - Scale Factors for Input
      1.000000      1.000000      1.000000      57.2978
!21 GRAVOUT RHOOUT LENOUT ANGOUT - Scale Factors for Output
      1.000000      1.000000      1.000000      57.2978
!22 GSHIFT(3), GORIG(3), GROT(3) - Input geometry transformation
      0.0 0.0 0.0
      0.0 0.0 0.0
      0.0 0.0 0.0
!23 SMA = Ship mass, SMI(1,1),(2,1),(3,1),(1,2)...(3,3) Mom. of Inertia
      .005715
      .000040      .000000      .000000
      .000000      .00035719      .000000

```

```

      .000000      .000000      .00035719
!24 RGRAV = center of gravity in input system
      0.0 0.0 -.0051843
!25 SYMGEO= 1 for Symmetry in calc., SYMINP =1 for symmetry in input
!25 SYMGEO,SYMINP
      0      1
!26 NCOMP0 ...
      1
!26 (cont) KCTYPE0 NEWL0 KSPWL0 SPWL0 NEWST0 KSPST0 SPST0,1->NCOMP0
      0      7      1      .000000      26      4      .500000
!27 IVM, IHM, ITM, NBKA, NBMX ...
      1      0      0      1      20
!27 (cont) XMC(123,1->NBKA)
      .000000      .000000      -.0051843
!27 (cont) XMS(123,I), AMS(I), AIS(123,I), DWS(I), AWS(I), EWS(I), (I=1-
>NBMX)
      .475 0.0 -.0051843 .000035 0.0 0.0 0.0 0.0 0.0 0.0
!28 IVISC
      1
!29 KINVIS
      2.8176E-10
!30 NFIN - Number of wing-like appendages (e.g. rudder, fins)
      1
!30 (cont) Values for one wing-like appendage - rudder
      0.504 0.0 -0.0255
      0.0 0.0 -1.0
      1.0 0.0 0.0
      .0485 .025 0.0
!31 NBK - Number of plate-like appendages (e.g. bilge keels)
      2
      -0.0424 0.0714 -0.0558
      0.0 0.707 -0.707
      -1.0 0.0 0.0
      0.002856
      0.25
      -0.0424 -0.0714 -0.0558
      0.0 -0.707 -0.707
      -1.0 0.0 0.0
      0.002856
      0.25

```

Appendix B: MOTSIM Source Code

```
*****
Program ship
*****
real dth,pmgg(6),t,accout(12),tol
integer istep,nstep,g,recdata
character*25 motfile

c *** Equation of Motion Vars
real meu1,meu2,meu3,omega1,omega2
real sma,ixx,k1,k2,k3,omegaw,fw
real h,h1
c *** Mass Motion VARS
real m,zm,factor,zeta,d,d2,dd2,dmax,d2max
real yip1(4),yi(4),yim1(4),yim2(4),yim3(4)
real fip1(4),fi(4),fim1(4),fim2(4),fim3(4)
real error(4),yc(4),yn(4),F(4),E(4),yip1p(4)

C *** Vars for Ship Eq. of motion & Forcing Function
meu2 = 2.56e-7
meu3 = -0.05*meu2
omega2 = 0.8925
sma = 0.005715
ixx = 0.00004
k2 = omega2**2*ixx
k3 = 0.05*k2
omegaw = 0.8925
fw = 6.0e-7
g = 1.0
dth = 0.04
nstep = 24000
tol = 0.00001
c vars for predictor corrector
h = 1.33333333*dth
h1 = 3.0*dth
c *** Mass Motion Vars (subscripts 1)
m = 0.02*sma
zm = -0.04
factor = 0.5
zeta = 0.005
omega1 = factor* (1.0/ (1.0+m/sma) ) *omega2
meu1 = 2*omega1*zeta
k1 = m*omega1**2
c zero arrays
call zero(yip1,4)
call zero(yi,4)
call zero(yim1,4)
call zero(yim2,4)
call zero(yim3,4)
call zero(fip1,4)
call zero(fi,4)
call zero(fim1,4)
call zero(fim2,4)
call zero(fim3,4)
call zero(error,4)
call zero(yc,4)
call zero(yn,4)
call zero(F,4)
call zero(E,4)
```

```

call zero(yiplp,4)
call zero (accout, 12)
call zero(pmgg,6)
ittflag = 0
c *****Initial Conditions and maximum values *****
d1    = 0.00
d2    = 0.00
dmax  = 0.14
d2max = 0.258
pmgg(4)= 0.0
c pmgg(4)= 0.262
accout(10) = 0.0
c
C *** Input file names for output
Print *, 'Enter name of Motion file'
read '(A)',motfile
Do while (recdata.ne. 1.and.recdata.ne.2)
  Print *,'Save Run Variables? (1 = yes, 2 = no)'
  read '(i1)' ,recdata
end do

C *** Begin time loop
  do istep = 1,nstep
C
C
C *** Initialize mass.mot file and write initial conditions

  if (istep.eq.1) then
dd2=0.0
OPEN(UNIT=28, STATUS='NEW' , FILE=motfile)
if(recdata.eq.1) then
OPEN(UNIT=29,STATUS='OLD' ,FILE='C:\b\runvars.txt',
* ACCESS='APPEND')
WRITE(29, '(A) ')motfile
WRITE(29, '(A)') ' m      dth      meu1      omegal      meu2      '//
*      ' omega2      zm'
WRITE(29, '(8g10.4)')m,dth,meu1,omegal,meu2,omega2,zm
WRITE(29,'(A)')' fw omegaw phi   phidot'
WRITE(29,' (8g10.4) ')fw, omegaw, pmgg(4), accout(10)
WRITE(29,*)
close(29)

      endif

yim3(1) = d1
yim3(2) = d2
yim3(3) = pmgg(4)
yim3(4) = accout(10)
t      = 0.0
call Fun(fim3,yim3,meu1,meu2,omegal,omegal,alpha,beta,g
* ,zm,t,fw,omegaw,k1,k2,ixx,m,meu3,k3)
write(28,'(8g11.4)')t,yim3(3) ,yim3(4) ,fim3(4) ,yim3(1),
*      yim3(2) ,fim3(2) ,ittflag

endif

C For t = delta t
if (istep.eq.2) then
do 10 j=1,4
  yim2(j) = yim3(j)+fim3(j)*dth
10  continue
  call Fun(f im2,yim2,meu1,meu2,omegal,omega2,alpha,beta,g
* ,zm,t,fw,omegaw,k1,k2,ixx,m,meu3,k3)
  write(28, ' (8g11.4) ')t,yim2(3),yim2(4),fim2(4),yim2(1),

```

```

* yim2(2) ,fim2(2),ittflag
endif
C For t = 2 delta t
  if (istep.eq.3) then
    do 20 j=1,4
      yim1(j) = yim2(j)+fim2(j)*dth
20    continue
      call Fun(f im1,yim1,meu1,meu2,omegal,omega2,alpha,beta,g
*           ,zm,t,fw,omegaw,k1,k2,ixx,m,meu3,k3)
      write(28,'(8g11.4)')t, yim1(3), yim1(4), fim1(4) ,yim1(1),
* yim1(2) ,fim1(2) ,ittflag
    endif
C For t = 3 delta t
  if (istep.eq.4) then
    do 30 j =1,4
      yi(j) = yim1(j)+fim1(j)*dth
30    continue
      callFun(fi,yi,meu1,meu2,omegal,omega2,alpha,beta,g
*           ,zm,t,fw,omegaw,k1,k2,ixx,m,meu3,k3)
      write(28,'(8g11.4)') t,yi(3),yi(4),fi(4),yi(1),
*           yi(2),fi(2),ittflag
    endif

C For Time step > 4
  if(istep.gt.4) then

C    Predict, save values
  ittflag = 1
  do 40 j=1,4
    yiplp(j) = yim3(j)+h*(2.0*fi(j)-fim1(j)+2.0*fim2(j))
    yipl(j) = yiplp(j) + 12.444444444444*error(j)
40  continue
C    correct the modified predicted solution and save first itt. values
100 call Fun(f ipl,yipl,meu1,meu2,omegal,omegal,alpha,beta,g,
*   zm,t,fw,omegaw,k1,k2,ixx,m,meu3,k3)
  do 50 j= 1,4
    yn(j) =0.125*(9.0*yi(j)-yim2(j) +h1*(fipl(j)+2.0*fi(j)-fim1(j)))
50  continue
C    increase itteration counter
  ittflag = ittflag + 1
c    check for convergence & save itt. values,
C    if not converged go to Correction step
  diffsum =abs((yn(1)-yipl(1))/yn(1))+abs((yn(2)-yipl(2))/yn(2))
* +abs((yn(3)-yipl(3))/yn(3))+abs((yn(4)-yipl(4))/yn(4))
  yipl = yn
  if(diffsum.gt.tol) goto 100
C    calculate error and make final corrections
  call Err (error, yipl , yiplp)
  do 60 j=1,4
    yipl(j) = yipl(j) - error(j)
60  continue
c*** check for max deflection ond vel of mass
  if(yipl(1).gt.dmax) yipl(1) = dmax
  if(yipl(1).lt.-dmax) yipl(1) =-dmax
  if(abs(yipl(1)).eq.abs(dmax)) yipl(2) = 0.0
C*** Set vars for next time step and save what is needed
  call Fun(fi1,yipl,meu1,meu2,omegal,omega2,alpha,beta,g,
*   zm,t,fw,omegaw,k1,k2,ixx,m,meu3,k3)
  fim2 = fim1
  fim1 = fi
  fi = fipl
  yim3 = yim2
  yim2 = yim1

```

```

    yim1 = yi
    yi = yipl
    write(28, ' (8g11.4) ')t,yipl(3) ,yipl(4) ,fipl(4) ,yipl(1),
*           yipl(2) ,fipl(2) ,ittflag
endif
t = t+dt
enddo
Print *, 'Run Ended Successfully'
end

C *****
subroutine Fun( f,y,meu1,meu2 ,omegal,omega2 , alpha,beta,g,
* zm,t, fw,omegaw,k1,k2, ix,m,meu3,k3)
C *****
double precision y(4),f(4)
real meu1,meu2,omegal,omega2,omegaw,alpha,beta,g,zm,t,k1,k2,ix,m
real meu3,k3
f(1) = y(2)
f(2) = - omega**2*y(1)-meu1*y(2)+g*sin(y(3))-zm*f(4)
f(3) = y(4)
f(4) = (1.0/(ix+m*y(1)**2+m*zm**2))*(-k2*y(3)-meu2*y(4)
*      -k3*y(3)**3-meu3*f(3)*abs(y(3))
*      +m*(zm*y(1)*f(3)**2-2*f(3)*y(1)*f(1)-g*zm*y(3))
*      +fw*cos(omegaw*t)+m*zm*f(2))
return
end
C *****
subroutine Err(e,y,y0)
double precision y0(4),y(4),e(4)
e(1) = 0.07438016528926*(y(1)-y0(1))
e(2) = 0.07438016528926*(y(2)-y0(2))
e(3) = 0.07438016528926*(y(3)-y0(3))
e(4) = 0.07438016528926*(y(4)-y0(4))

end

```

Appendix C: LAMP Non-Dimensionalization Chart

| Values | Metric | British | Nondimensional |
|-------------------------|------------------------|----------------------------|---|
| ρ | 1025 kg/m ³ | 1.991 slug/ft ³ | 1.0 |
| g | 9.8 m/sec ² | 32.2 ft/sec ² | 1.0 |
| L | LBP, m | LBP, ft | 1.0 |
| α | 57.29578 (degrees) | 57.29578 (degrees) | 1.0 (radians) |
| Mass | kg | slugs | $\rho \cdot L^3$ |
| Force | N | pounds | $\rho \cdot g \cdot L^3$ |
| Moment | N-m | ft-pounds | $\rho \cdot g \cdot L^4$ |
| Pressure | N/m ² | pounds/ft ² | $\rho \cdot g \cdot L$ |
| Time | seconds | seconds | $\sqrt{\frac{L}{g}}$ |
| Volume | m ³ | ft ³ | L^3 |
| Moment of Inertia | kg-m ² | slug-ft ² | $\rho \cdot L^5$ |
| Frequency | rad/sec | rad/sec | $\text{rad} \cdot \sqrt{\frac{g}{L}}$ |
| Period | sec | sec | $\sqrt{\frac{L}{g}}$ |
| Positions, Lengths | m | ft | L |
| Linear Velocity | m/sec | ft/sec | $\sqrt{g \cdot L}$ |
| Linear Acceleration | m/sec ² | ft/sec ² | g |
| Angles Motion | degrees | degrees | radians |
| Angular Velocity | deg/sec | deg/sec | $\text{rad} \cdot \sqrt{\frac{g}{L}}$ |
| Angular Acceleration | deg/sec ² | deg/sec ² | $\text{rad} \cdot \frac{g}{L}$ |
| Kinematic Viscosity | m ² /sec | ft ² /sec | $\sqrt{g \cdot L^3}$ |
| Impulse Response Mass | kg/sec | slug/sec | $\rho \cdot L^3 \cdot \sqrt{\frac{g}{L}}$ |
| Impulse Response Moment | kg-m ² /sec | slug-ft ² /sec | $\rho \cdot L^5 \cdot \sqrt{\frac{g}{L}}$ |
| Young's Modulus | N/m ² | pounds/ft ² | $\rho \cdot g \cdot L$ |

VITA

Thomas W. Treakle, III was born on October 10, 1964 in Norfolk Virginia. After high school he worked in the marine construction industry, had a Virginia real estate license, and was a self employed mechanical contractor. In May 1995 he earned a B.S. in Ocean Engineering at Virginia Polytechnic Institute and State University. He obtained his M.S. in Ocean Engineering in May 1998 also from Virginia Polytechnic Institute and State University. During his masters study, he worked as a teaching assistant on several undergraduate ocean engineering classes and performed research for the MURI on Nonlinear Control of Dynamical Systems funded by the Office of Naval Research. His major area of interest is Computational Ship Motions and Loads. He is currently working as a Research Engineer at SAIC, Ship Technology Division in Annapolis Maryland.